Journal of Medicinal Chemistry

Article

pubs.acs.org/jmc

Extending the Structure–Activity Relationship of Anthranilic Acid Derivatives As Farnesoid X Receptor Modulators: Development of a Highly Potent Partial Farnesoid X Receptor Agonist

Daniel Merk,*[,†] Christina Lamers,[†] Khalil Ahmad,[†] Roberto Carrasco Gomez,[†] Gisbert Schneider,[‡] Dieter Steinhilber,[†] and Manfred Schubert-Zsilavecz[†]

[†]Institute of Pharmaceutical Chemistry, Goethe University Frankfurt, Max-von-Laue-Strasse 9, 60438 Frankfurt, Germany

[‡]Department of Chemistry and Applied Biosciences, ETH Zürich, Vladimir-Prelog-Weg 1-5/10, 8093 Zürich, Switzerland

Supporting Information

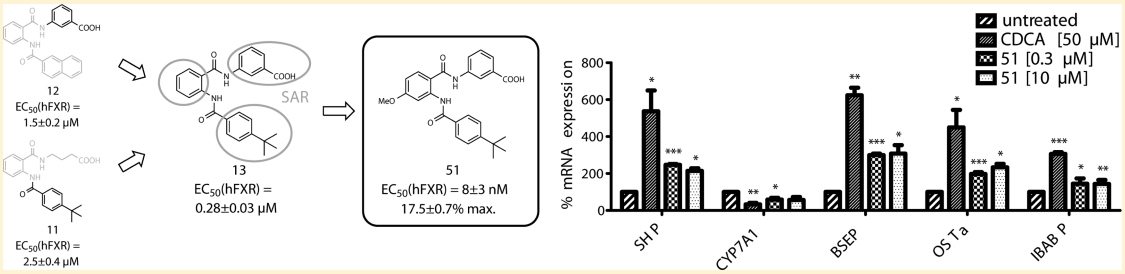

ABSTRACT: The ligand activated transcription factor nuclear farnesoid X receptor (FXR) is involved as a regulator in many metabolic pathways including bile acid and glucose homeostasis. Therefore, pharmacological activation of FXR seems a valuable therapeutic approach for several conditions including metabolic diseases linked to insulin resistance, liver disorders such as primary biliary cirrhosis or nonalcoholic steatohepatitis, and certain forms of cancer. The available FXR agonists, however, activate the receptor to the full extent which might be disadvantageous over a longer time period. Hence, partial FXR activators are required for long-term treatment of metabolic disorders. We here report the SAR of anthranilic acid derivatives as FXR modulators and development, synthesis, and characterization of compound **51**, which is a highly potent partial FXR agonist in a reporter gene assay with an EC_{50} value of 8 ± 3 nM and on mRNA level in liver cells.

INTRODUCTION

As a ligand activated transcription factor, nuclear farnesoid X receptor (FXR) regulates several metabolic pathways involved in bile acid, triglyceride, and glucose homeostasis. It binds to specific response elements on the DNA as monomer or as heterodimer with RXR and controls the transcription of genes especially involved in bile acid synthesis and metabolism when activated by its physiological ligands, the bile acids.[1,2]

Modulation of FXR may be a valuable therapeutic approach for various pathophysiological conditions. FXR activation showed promising results in vitro and in vivo for the treatment of metabolic,[3−8] neoplastic,[9] as well as inflammatory[10−15] diseases such as diabetes and inflammatory bowel disease. Clinical development of FXR agonists for the treatment of the liver disorders primary biliary cirrhosis (PBC), nonalcoholic steatohepatitis (NASH), and nonalcoholic fatty liver disease (NAFLD) is ongoing.[6,16,17] Most recently, an in vivo model indicated that the very beneficial metabolic effects of vertical sleeve gastrectomy in adipose individuals could be due to activation of FXR.[18]

A number of synthetic steroidal and nonsteroidal FXR agonists has been developed so far (reviewed in ref 19). By introduction of an additional ethyl residue in the most potent physiological FXR ligand chenodeoxycholic acid (CDCA, **1**, Scheme 1), 6α-ethyl-CDCA[20] (6-ECDCA, obeticholic acid, INT-747, **2**, Scheme 1) was discovered, which is presently being investigated in clinical phase II and III trials for PBC, NASH, and NAFLD.[17] The most important and widely used nonsteroidal FXR agonist is GW4064[21] (**3**, Scheme 1), which served as a model or reference compound in many experiments. **3** and several other synthetic nonsteroidal FXR agonists, however, have a poor bioavailability or show toxic effects which limit their clinical utility.[19,22−25] In addition, a recent study indicated that GW4064 (**3**) is active on several off-targets.[26]

CDCA (**1**), 6-ECDCA (**2**), and GW4064 (**3**) all constitute full FXR agonists. For GW4064 (**3**), the EC_{50} value varies in literature depending on the applied test system from 15 nM in a coactivator recruitment assay to 0.9 μM in a reporter gene assay. 6-ECDCA (**2**) was characterized with an EC_{50} value of 99 nM for coactivator recruitment and 85 nM in a reporter gene assay (reviewed in ref 27).

Given the fact that conditions which might be treatable with FXR ligands are predominantly metabolic diseases that require

Received: June 20, 2014

 © XXXX American Chemical Society dx.doi.org/10.1021/jm500937v | J. Med. Chem. XXXX, XXX, XXX−XXX

Scheme 1. Important FXR Agonists CDCA (1), 6-ECDCA (2), and GW4064 (3)

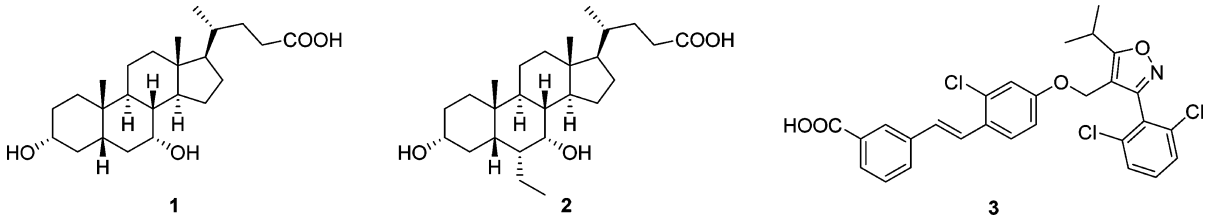

Scheme 2. Synthesis Routes for Preparation of the Tested Acylanthranilic Amides

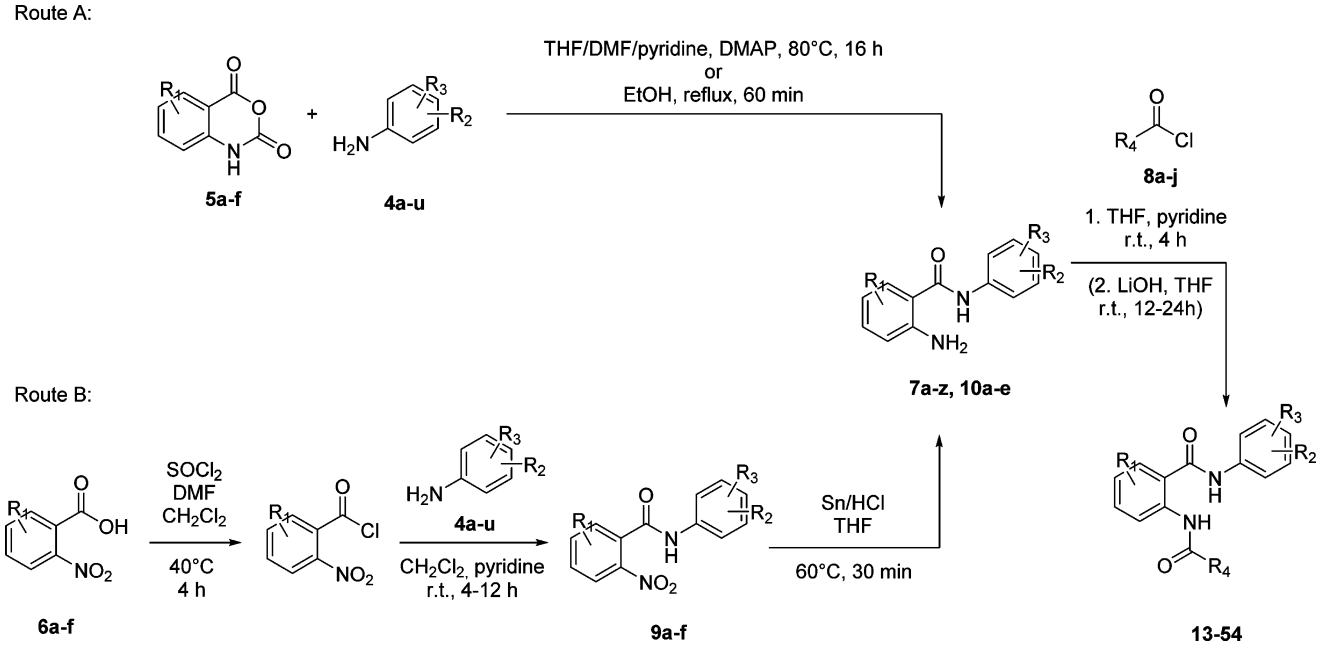

a stable long-term therapy, well tolerated agents are required that can be applied over long time. Many of the known FXR ligands, however, exhibit toxicity and show poor bioavailability.[19,22−25] In addition, targeting of nuclear receptors involved in metabolic processes such as FXR and PPARγ has taught that full activation of a ligand activated transcription factor may lead to various side effects in long-term treatment and that full activation is not necessarily required for beneficial effects.[25] New potent FXR modulators are therefore needed that do not exhibit full agonism but only activate the nuclear receptor to a partial extent.

We recently described the discovery and development of anthranilic acid derivatives as novel FXR agonists.[28,29] Here we report the optimization of the anthranilic acid scaffold to highly potent FXR partial agonists by structure−activity relationship (SAR) studies and molecular docking. Optimized compound **51** constitutes a potent partial FXR agonist with an EC_{50} value of 8 ± 3 nM and a maximum relative FXR activation of 17.5 ± 0.7% in a FXR reporter gene assay.

RESULTS

Chemistry. Anthranilic acid derivatives were generated via two different synthetic strategies depending on the reactivity and availability of starting materials.

Synthetic route A involved the *ortho*-aminobenzoylation of an aniline derivative (**4a−u**) with a derivative of isatoic anhydride (**5a−f**) to introduce the acidic headgroup at the anthranilic acid core structure. We previously reported this *ortho*-aminobenzoylation of amines or anilines in a mixture of DMF and pyridine at 80 °C and in the presence of 4-DMAP as a catalyst.[28] For several substituted anilines that were necessary for our SAR, these conditions however led to very poor yields. Better yields could be achieved when the reaction was carried out in absolute ethanol under reflux with an excess of the isatoic anhydride derivative (**5a−f**). The better performance of this reaction in ethanol may probably be due to better solubility and the presence of a protic solvent (Scheme 2).

For some aniline derivatives as headgroup substituents that showed a very poor nucleophilicity, another synthetic strategy was necessary. In addition, some isatoic anhydride derivatives containing certain substituents were not commercially available. In these cases, synthetic route B was used.

Synthetic route B started with *ortho*-nitrobenzoic acid derivatives (**6a−f**), which were activated by chlorination with thionyl chloride in methylene chloride in the presence of catalytic amounts of DMF and subsequently reacted with the respective aniline derivatives (**4a−u**) in THF/pyridine to introduce the headgroup substituents. By reduction of the nitro group of the resulting derivatives **9a−f** with tin and hydrochloric acid in THF, the required *ortho*-aminobenzoylaniline derivaties (**7a−z, 10a−e**) were available (Scheme 2).

Finally, the *ortho*-aminobenzoylaniline derivatives **7a−z** and **10a−e** from route A or B were reacted with various acyl chlorides (**8a−j**) to introduce the acyl substituent at the aniline group of the anthranilic acid core structure. For some compounds, a final alkaline ester hydrolysis was necessary

dx.doi.org/10.1021/jm500937v | J. Med. Chem. XXXX, XXX, XXX−XXX

Scheme 3. Synthesis of Tetrazole Derivative 27 and Amide 28

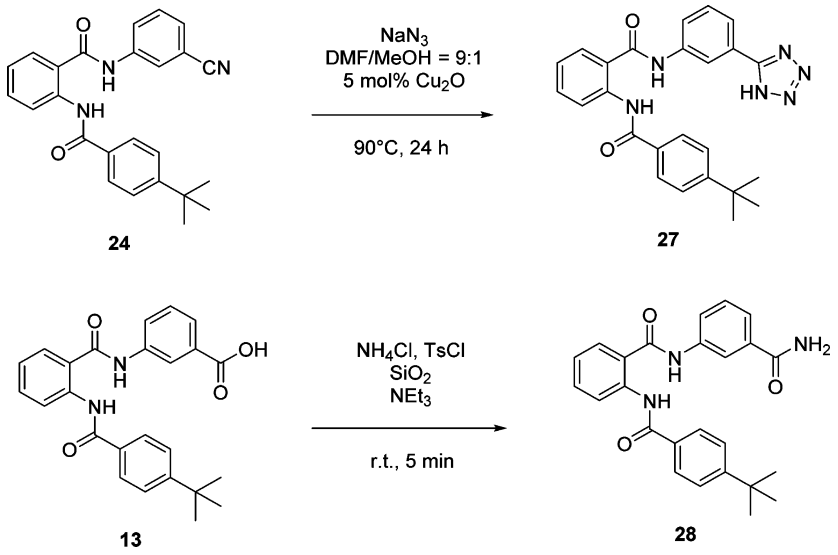

Scheme 4. Development of Compound 13

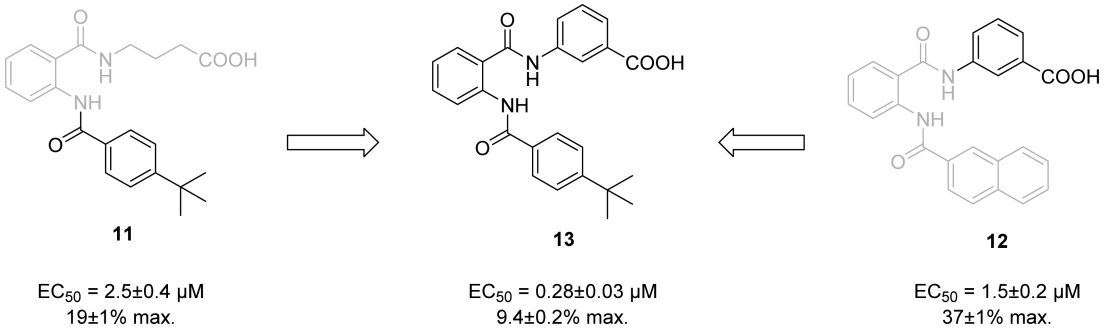

after this synthesis procedure to yield the test compound (Scheme 2).

The bioisosteric derivatives **27** and **28** were generated by different strategies. Tetrazole derivative **27** was obtained by cycloaddition of sodium azide and nitrile **24** in DMF/MeOH in the presence of catalytic amounts copper(I) oxide.[30] For the preparation of amide **28**, the respective carboxylic acid derivative **13** was used as starting material and reacted with silica supported ammonium chloride in the presence of tosyl chloride and triethyl amine as described previously[31] (Scheme 3).

Biological Evaluation and Structure–Activity Relationships. In our first SAR study, we discovered compounds **11** (EC_{50} = 2.5 ± 0.4 μM, 19 ± 1% max) and **12** (EC_{50} = 1.5 ± 0.2 μM, 37 ± 1% max) as FXR partial agonists with moderate potency. Recombination of the 3-aminobenzoic acid of **12** as headgroup and the 4-*tert*-butylbenzoyl moiety of **11** as lipopholic acyl substituent in compound **13** resulted in improved potency and provided the starting point of this SAR study (**13**, EC_{50} = 0.28 ± 0.03 μM, 9.4 ± 0.2% max, Scheme 4). With compound **13** as the starting point, we investigated the SAR of the lipophilic acyl substituent, the acidic headgroup, and the anthranilic acid core structure.

FXR activity was determined in a full-length FXR reporter gene assay in HeLa cells that were transiently transfected with hFXR (constitutively expressed, CMV promoter), hRXR (constitutively expressed, CMV promoter), a firefly luciferase (reporter gene) under the control of a minimum BSEP promoter, and a constitutively expressed renilla luciferase with SV40 promoter as internal control for transfection efficiency and toxicity. As reference compound, GW4064 (**3**) was used in a concentration of 3 μM, which we set as 100% FXR activation. The assay was validated with CDCA (**1**), which had an EC_{50} of 18 ± 1 μM with 88 ± 3% maximum relative FXR activation and 6-ECDCA (**2**), which showed an EC_{50} of 0.16 ± 0.02 μM (87 ± 3% max).

We first analyzed fragments of the lead compound **13** to evaluate the possibility of reducing the size of the compounds. Fragment **7a** without lipophilic acyl substituent and anthranilic acid were inactive, however. We then inverted both amide bonds of compound **13**, resulting in **14**, which was inactive on FXR as well.

In case of the lipophilic acyl substituent, the SAR was equally steep as we have already observed in our first SAR study.[28] Replacement of the 4-*tert*-butyl moiety of **13** by comparably large and lipophilic residues such as a trifluoromethyl group (**15**) or a bromine atom (**16**) strongly reduced the potency. In our first SAR study, also a 2-naphthoyl substituent (**12**) showed potent FXR activating results. We therefore investigated potential bioisosters and homologues of this moiety. A methylenedioxo residue (**17**), a dihydrobenzodioxine residue (**18**), and a 4-trifluoromethyl-3-fluorobenzyl moiety (**19**) were significantly less active than the 2-naphthoyl substituent (**12**). Moving the substitution from 4-position of the aromatic ring to 3- and 5-positions in **20** or the introduction of additional carbon atoms between amide group and aromatic ring in **21**

dx.doi.org/10.1021/jm500937v | J. Med. Chem. XXXX, XXX, XXX–XXX

Table 1. In Vitro Activities of 7a and 13−22 in the Full-Length FXR Transactivation Assay[a]

#	R	EC_{50} [μM] (max. rel. activation [%])	#	R	EC_{50} [μM] (max. rel. activation [%])
13	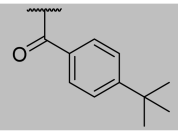	0.28±0.03 (9.4±0.2)	**18**	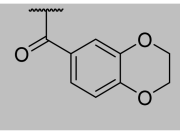	4.9±0.4 (23.3±0.4)
7a	H	i.a. (30 μM)	**19**	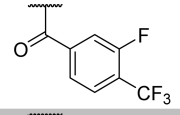	5.0±0.2 (32.4±0.5)
15	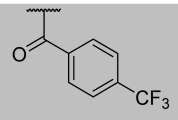	6.9±0.2 (26.2±0.4)	**20**	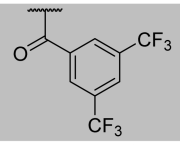	i.a. (30 μM)
16	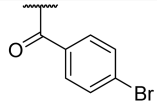	3.7±0.9 (14.3±0.9)	**21**	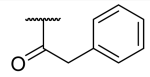	i.a. (30 μM)
17	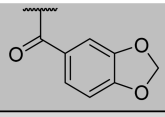	10.0±0.2 (12.2±0.5)	**22**	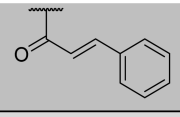	5.2±0.9 (15.6±0.5)
14	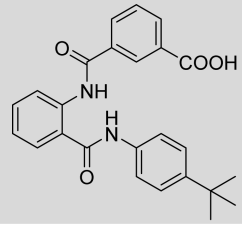				i.a.

[a]Values are expressed as mean ± SEM. i.a.: inactive.

and **22** reduced potency as well. Summarizing the above, the 4-*tert*-butylbenzoyl moiety of lead compound **13** proved to be the best substituent in this position (Table 1).

As next step, we investigated the SAR of the acidic headgroup. Therefore, we replaced the carboxylic acid with suitable bioisosters of the carboxylic acid and introduced additional carbon atoms between aromatic ring and carboxylic acid. Bioisosteric replacement of the carboxylic acid with a methyl ketone (**23**), a nitrile group (**24**), a methoxy group (**25**), or a methylmercaptan moiety (**26**) did not significantly change the potency of the compounds. A 1*H*-tetrazolyl moiety (**27**) as headgroup significantly enhanced the maximum relative activation activity at FXR, but the EC_{50} value was worsened by a factor 10. Replacement of the carboxylic acid by a carboxylic amide (**28**) improved the potency at FXR, but unfortunately the compound was quite toxic to the HeLa cells in our assay system, so we did not further investigate the amide moiety. The potency could also be improved by introduction of a second methoxy group as hydrogen bond acceptor in 2-position of the aromatic ring (**29**), while a third methoxy group (**30**) completely disrupted activity (Table 2).

By replacing the benzoic acid residue of **13** with a phenyl acetic acid (**31**), potency was slightly lowered while a 3-phenlylpropionic acid (**32**) increased the activity on FXR (Table 2).

To discover additional space for further substituents in the binding pocket, we introduced additional residues at the aromatic ring of the headgroup. A methyl group in 6-position (**33**) disrupted FXR activation activity, while a methyl group on either side of the carboxylic acid in 2- and 6-positions (**34** and **35**) strongly improved the potency of the compounds. Because docking of compound **13** into the FXR ligand binding site had suggested additional space for substituents in 4-position of the aromatic ring of the headgroup, we also investigated other residues than the methyl group (**33**), which was inactive. Introduction of a methoxy group (**36**), a fluorine (**37**), or chlorine atom (**38**) retained low FXR activating activity, but all compounds **36**−**38** showed lower potency than the lead compound. This worse activity might also be due to steric clashes between 4-substituent and the amide group, which makes the aromatic ring of the headgroup flip out of the plane of the central aromatic ring. This effect might however be generated by a larger substituent in the 2-position (compound **34**) as well (Table 3).

The best position for further substitution therefore seemed to be the 6-position (**35**) next to the carboxylic acid. We replaced the methyl group of **35**, which had strongly improved the potency of compound **13** by various other residues. However, the SAR was quite steep again. While the introduction of a methoxy group (**39**) retained the low

dx.doi.org/10.1021/jm500937v | J. Med. Chem. XXXX, XXX, XXX−XXX

Table 2. In Vitro Activities of 23−32 in the Full-Length FXR Transactivation Assay[a]

#	R	EC_{50} [μM] (max. rel. activation [%])	#	R	EC_{50} [μM] (max. rel. activation [%])
23	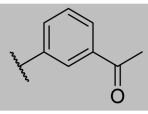	0.48±0.07 (18.8±0.5)	**28**	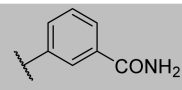	0.074±0.011 (14.8±0.3)
24	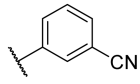	0.23±0.05 (17.5±0.8)	**29**	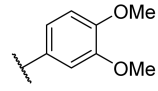	0.071±0.022 (12.7±0.2)
25	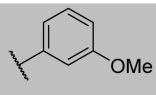	0.38±0.06 (13.3±0.7)	**30**	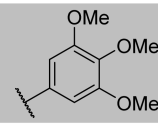	i.a. (30 μM)
26	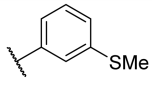	0.20±0.03 (8.6±0.3)	**31**	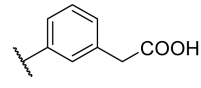	0.42±0.13 (26.4±1.4)
27	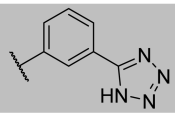	2.9±0.8 (39±4)	**32**	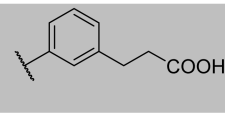	0.064±0.013 (21.8±0.6)

[a]Values are expressed as mean ± SEM. i.a.: inactive.

Table 3. In Vitro Activities of 33−42 in the Full-Length FXR Transactivation Assay[a]

#	R	EC_{50} [μM] (max. rel. activation [%])	#	R	EC_{50} [μM] (max. rel. activation [%])
33	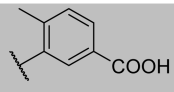	i.a. (30 μM)	**35**	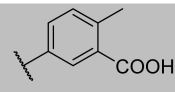	0.045±0.009 (22.4±0.5)
34	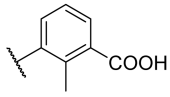	0.042±0.001 (19.0±0.2)	**39**	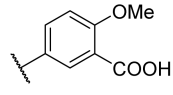	0.047±0.001 (19.1±0.5%)
36	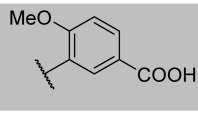	4.7±0.3 (14.9±0.2)	**40**	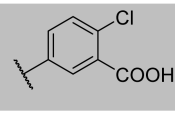	0.28±0.04 (18.7±0.4)
37	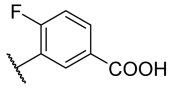	0.48±0.14 (12.0±0.4)	**41**	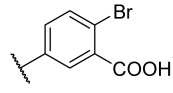	0.15±0.01 (16.4±0.2)
38	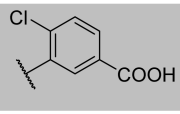	1.1±0.3 (15.6±0.7)	**42**	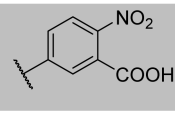	i.a. (30 μM)

[a]Values are expressed as mean ± SEM. i.a.: inactive.

dx.doi.org/10.1021/jm500937v | J. Med. Chem. XXXX, XXX, XXX−XXX

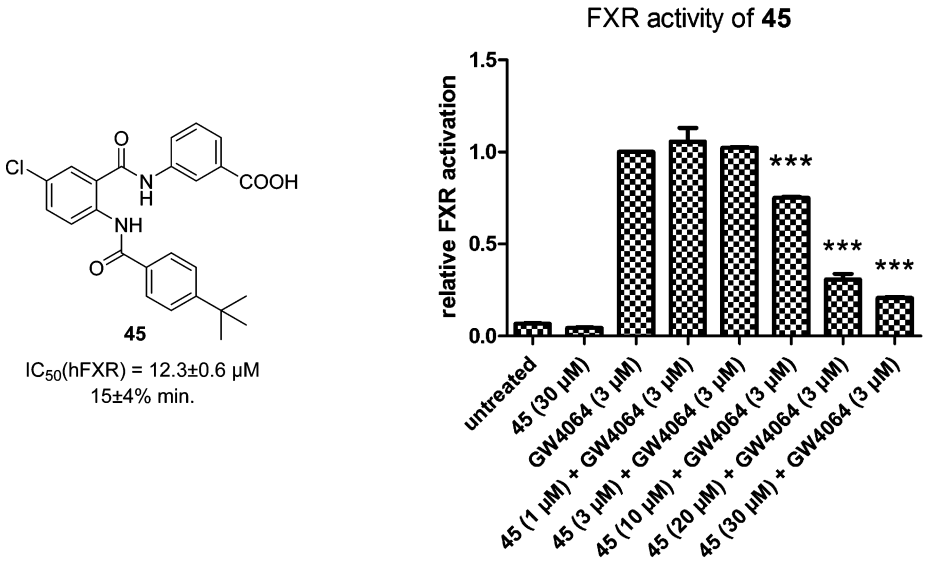

Figure 1. Antagonistic activity of **45** in competition with GW4064 (**3**) in the reporter gene assay. * $p < 0.05$; ** $p < 0.01$; *** $p < 0.001$.

Table 4. In Vitro Activities of 43−51 in the Full-Length FXR Transactivation Assay[a]

#	R_1 = COOH; R_2 = 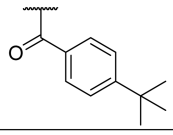	EC_{50} [μM] (max. rel. activation [%])	#	R_1 = COOH; R_2 = 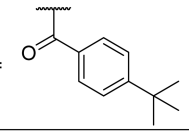	EC_{50} [μM] (max. rel. activation [%])
13	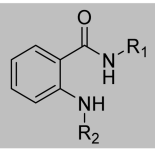	0.28±0.03 (9.4±0.2)	**47**	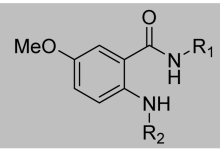	*antagonistic* IC_{50} = 15.1±0.1 μM (10±1% min.)
43	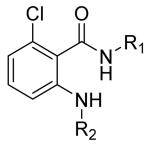	i.a. (30 μM)	**48**	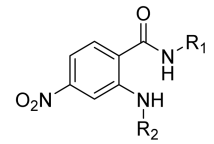	i.a. (30 μM)
44	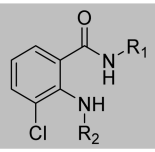	i.a. (30 μM)	**49**	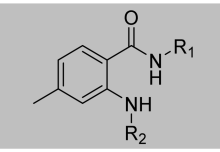	0.061±0.014 (21±1)
45	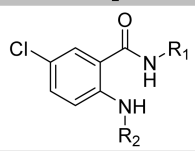	*antagonistic* IC_{50} = 12.3±0.6 μM (15±4% min.)	**50**	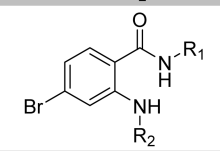	0.048±0.016 (15.4±0.9)
46	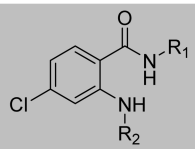	0.047±0.001 (19.1±0.5)	**51**	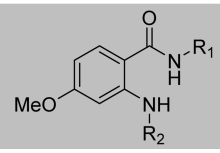	0.008±0.003 (17.5±0.7)

[a]Values are expressed as mean ± SEM. i.a.: inactive.

nanomolar activity of **35**, a chlorine (**40**) or bromine atom (**41**) reduced the potency by about 6-fold and 3-fold, respectively. Introduction of a nitro group (**42**) even completely disrupted the activity (Table 3).

dx.doi.org/10.1021/jm500937v | J. Med. Chem. XXXX, XXX, XXX−XXX

At last we also investigated the availability of additional space around the anthranilic acid core structure of lead compound **13** by introducing chlorine atoms in every position of the aromatic ring. An additional chlorine atom in 3- or 6-positions of the anthranilic acid moiety (**43** and **44**) led to inactivity on FXR, which might be due to steric clashes with the amide groups that causes a different geometry. Chlorine substitution in the 5-position (**45**) interestingly led to moderate antagonistic activity on FXR (Figure 1), while a chlorine atom in the 4-position (**46**) improved the agonistic activity (Table 4).

In the next step, we replaced the chlorine atom in 4-position of compound **46** with various other substituents. In this case, the SAR was less steep than before. While the 4-nitro derivative **48** was inactive, the 4-methyl (**49**) as well as the 4-bromo derivative (**50**) were more potent than the 4-chloro derivative **46**. Introduction of a methoxy group in 4-position (**51**) finally led to the desired improvement of potency to a low nanomolar EC_{50} value (Table 4).

To confirm the antagonistic activity of **45**, we prepared derivative **47** with a methoxy group in the 5-position which exhibited a comparable antagonistic activity. Further investigation of this antagonism shall, however, be performed and discussed elsewhere (Table 4).

Finally, we investigated the possibility to recombine the best moieties of our SAR studies to further improve the potency. Therefore, we tested derivative **52** containing the 4-chloro substituent at the anthranilic acid core and the 6-methyl residue at the headgroup. Although potent on FXR, this compound (**52**) could not outmatch the derivatives **35** and **46** with only one of the substituents but was more or less equally potent. When the best residues, in particular the 4-methoxy group at the central aromatic ring and the 6-methyl group at the headgroup aromatic ring, were combined in **53**, potency was even slightly diminished. We assumed this might be due to steric clashes with the receptor by the double substitution and prepared the smallest possible compound with two substitutions (**54**) which contained a 4-methyl group at the anthranilic acid residue and a 6-methyl substituent at the headgroup. However, this derivative was again equally potent as the derivatives bearing only one of the methyl groups (**35** and **49**). Hence, **51** remained the best anthranilic acid derivative as FXR agonist (Tables 3, 4, and 5).

In Vitro Characterization of Compound 51. To further investigate the FXR agonist activity of compound **51**, we determined its effect on FXR target genes in the liver carcinoma cell line HepG2 and the colorectal adenocarcinoma cell line HT-29 by quantitative PCR experiments at the concentrations 0.1, 0.3, 1, 3, and 10 μM. **51** showed statistically significant partial agonist activity on FXR target genes. The mRNA of small heterodimer partner (SHP) was induced by about 2-fold (untreated, 100%; CDCA, 537 ± 113%; **51**, 0.1 μM 239 ± 88%, 0.3 μM 247 ± 4%, 1 μM 181 ± 12%, 3 μM 185 ± 18%, 10 μM 214 ± 14%) and mRNA of CYP7A1 (untreated, 100%; CDCA, 33 ± 8%; **51**, 0.1 μM 52 ± 17%, 0.3 μM 59 ± 9%, 1 μM 55 ± 11%, 3 μM 67 ± 10%, 10 μM 57 ± 16%), which is not a direct FXR target gene but affected via SHP induction, was repressed by about 2-fold. Also on the organic solute transporter α (OSTα: untreated, 100%; CDCA, 450 ± 94%; **51**, 0.1 μM 151 ± 11%, 0.3 μM 198 ± 10%, 1 μM 140 ± 14%, 3 μM 149 ± 13%, 10 μM 234 ± 19%), the bile salt export protein (BSEP: untreated, 100%; CDCA 624 ± 40%; **51**, 0.1 μM 294 ± 16%; 0.3 μM 300 ± 8%; 1 μM 319 ± 46%; 3 μM 326 ± 58%; 10 μM 308 ± 46%; GW4064 (**3**, 3 μM) 1523 ± 187%), and the ileal bile acid binding protein (IBABP: untreated, 100%; CDCA, 288 ± 15%; **51**, 0.1 μM 188 ± 42%, 0.3 μM 145 ± 29%, 1 μM 161 ± 12%, 3 μM 168 ± 29%, 10 μM 144 ± 22%), **51** showed a concentration independent partial agonistic activity. For all investigated target genes, this effect reached a maximum of about 40% of the effect produced by CDCA (**1**, 50 μM). The fact that **51** exhibited a constant effect on the target genes in a concentration range from 0.1 to 10 μM shows that **51** has a partial FXR agonistic activity not only in the reporter gene assay but on FXR target genes on mRNA level as well (Figure 2).

Table 5. In Vitro Activities of 52−54 in the Full-Length FXR Transactivation Assay[a]

#	R =	EC_{50} [μM] (max. rel. activation [%])
52	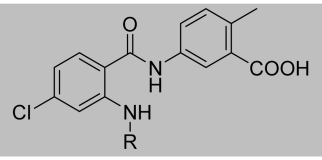	0.11±0.02 (20.1±0.5)
53	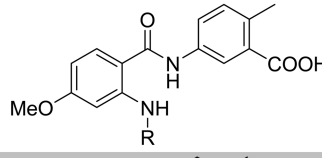	0.087±0.020 (22.3±0.7)
54	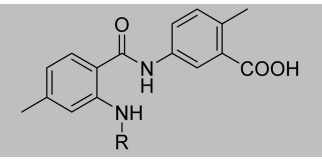	0.043±0.007 (16.8±0.3)

[a]Values are expressed as mean ± SEM. i.a.: inactive.

To characterize the pharmacological profile of **51**, we also investigated its activity on common off-targets. Compound **51** was inactive on the membrane bile acid receptor TGR5 (30 μM) and on PPARδ (3 μM). A slight activity on PPARγ and PPARα was observed (EC_{50}(PPARγ) = 2.99 ± 0.10 μM (81 ± 2% max); EC_{50} (PPARα) > 10 μM), which makes **51** about 375-fold selective for FXR over PPARγ and >1000-fold over PPARα, PPARδ, and the membrane bile acid receptor TGR5 (Figure 3A).

Furthermore, **51** showed an aqueous solubility of 2.6 mg/L and was quite stable against metabolism by liver microsomes in vitro. After 60 min incubation, 80.2 ± 0.2% of the compound were still detectable (Figure 3B).

Finally, we determined the toxicity of compound **51** which showed slight toxic effects on HeLa cells in the reporter gene assay starting from 30 μM. In HepG2 cells, **51** had an antiproliferative effect at concentrations of 30 μM and above in a WST-1 assay and exhibited acute toxicity at the same concentrations in an LDH assay (Figure 3C,D).

Receptor−Ligand Docking. Among the 25 available cocrystal structures of the FXR-LBD, the complex (PDB ID: 3OLF[32]) with the benzimidazole-based partial agonistic ligand **55** (EC_{50} = 0.5 μM, 51% max)[32] seemed most suited for docking studies on the here reported partial FXR agonists. Comparison of benzimidazole-based cocrystal structures (complexes of **55** (3OLF) and related derivatives (PDB IDs:

dx.doi.org/10.1021/jm500937v | J. Med. Chem. XXXX, XXX, XXX−XXX

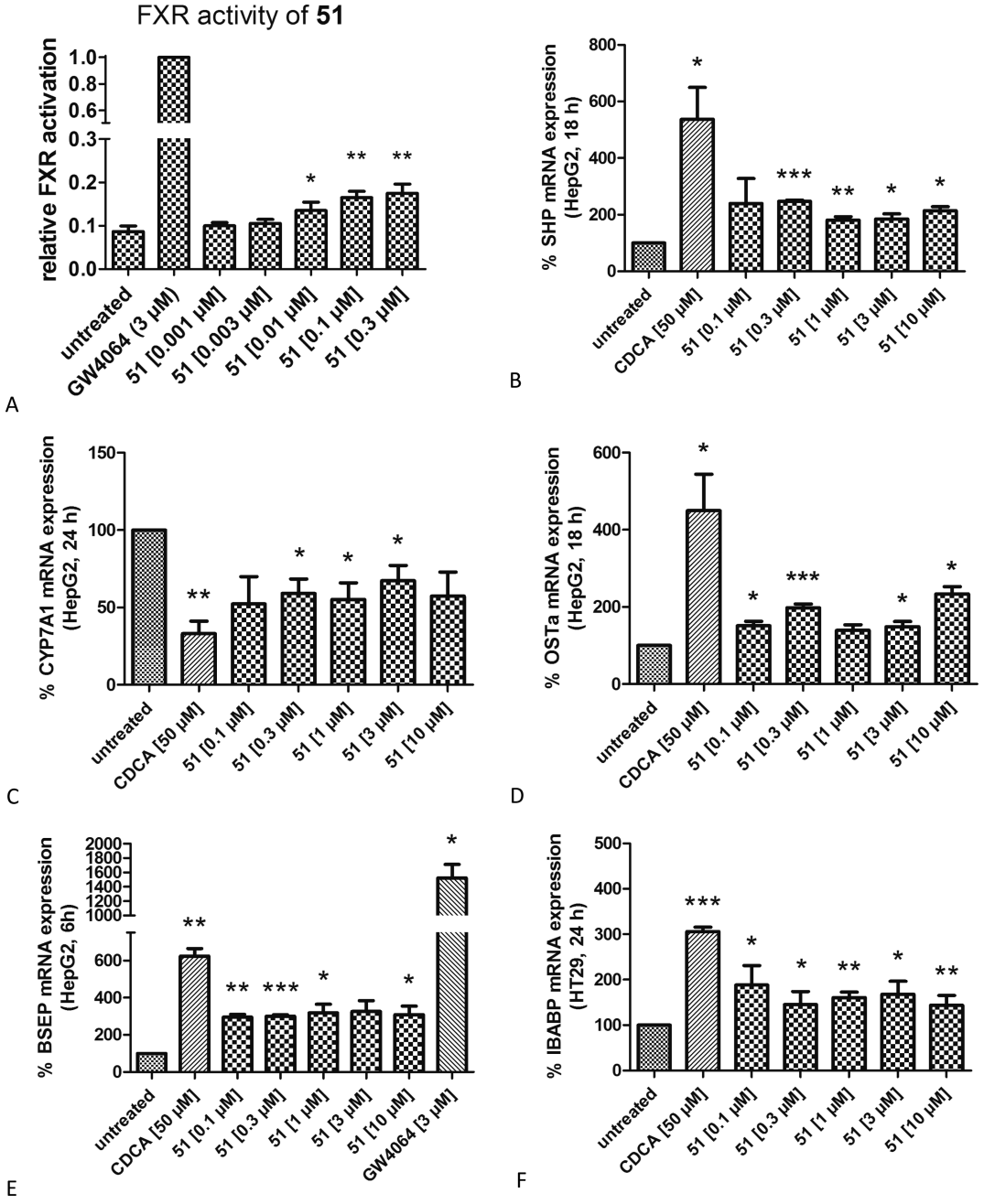

Figure 2. In vitro pharmacological activity of compound **51**. (A) Relative FXR activation of 51 in the reporter gene assay compared to 3 μM GW4064 (**3**), which is set as 100%. Nonlinear regression yielded an EC_{50} value of 8 $\pm$ 3 nM with 17.5% max rel activation; n = 5. (B) Effect of **51** on mRNA expression of direct FXR target gene SHP in HepG2 cells. Partial FXR agonist **51** (0.1, 0.3, 1, 3, 10 μM) induces SHP expression by about 2-fold (physiologic FXR agonist CDCA: 5.4-fold); effect independent from concentration; n = 4. (C) Effect of **51** (0.1, 0.3, 1, 3, 10 μM) on mRNA expression of indirect FXR target gene CYP7A1 in HepG2 cells. Partial FXR agonist **51** represses CYP7A1 expression to about 60% (physiologic FXR agonist CDCA: 33%); effect independent from concentration; n = 4. (D) Effect of **51** (0.1, 0.3, 1, 3, 10 μM) on mRNA expression of direct FXR target gene OSTα in HepG2 cells. Partial FXR agonist **51** induces OSTα expression by about 1.8-fold (physiologic FXR agonist CDCA: 4.5-fold); effect independent from concentration; n = 4. (E) Effect of **51** (0.1, 0.3, 1, 3, 10 μM) on mRNA expression of direct FXR target gene BSEP in HepG2 cells. Partial FXR agonist **51** induces BSEP expression by about 3-fold (physiologic FXR agonist CDCA, 6.5-fold; GW4064, 15-fold); effect independent from concentration; n = 4. (F) Effect of **51** (0.1, 0.3, 1, 3, 10 μM) on mRNA expression of direct FXR target gene IBABP in HT-29 cells. Partial FXR agonist **51** induces IBABP expression by about 1.7-fold (physiologic FXR agonist CDCA: 3-fold); effect independent from concentration; n = 4. * $p < 0.05$; ** $p < 0.01$; *** $p < 0.001$.

3OKH, 3OKI, 3OMK, 3OMM, 3OOF, 3OOK)) with the cocrystal structure of the GW4064-analogue **56** (PDB-ID: 3RUT[33]) revealed significant differences in the protein structure and in the form of the ligand binding pocket (Figure 4A). Especially, the helices 3 and 7 which form the ligand binding pocket are in significantly shifted positions. This influences the geometry of the ligand binding site. While the complexes of the partial agonistic benzimidazoles such as **55** reveal a triangular ligand binding pocket, the pocket of full agonistic ligands such as **56** is long and narrow. Docking of the here reported partial agonistic anthranilic acid derivatives in a model of the FXR-LBD derived from 3OLF[32] yielded sound

dx.doi.org/10.1021/jm500937v | J. Med. Chem. XXXX, XXX, XXX−XXX

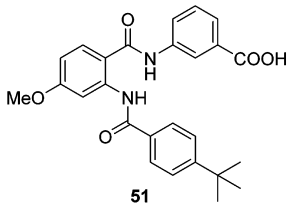

51

EC_{50}(hFXR) = 8±3 nM (17.5±0.7%); pEC_{50} = 8.1

molecular weight: 446
aqueous solubility: 2.6 mg/L; ***clogP***: 4.95
tPSA: 104.7;
H-bond donors: 3; ***H-bond-acceptors***: 7
LE: 0.24; ***SILE***: 2.83

selective over PPARs and membrane BA rec. TGR5 (***PPARα***: EC_{50} > 10 μM (not determined due to toxicity), selectivity > 1000-fold; ***PPARγ***: EC_{50} = 2.99±0.10 μM (81±2% max.), selectivity ~375-fold; ***PPARδ***: inactive (3 μM); ***TGR5***: inactive (30 μM))

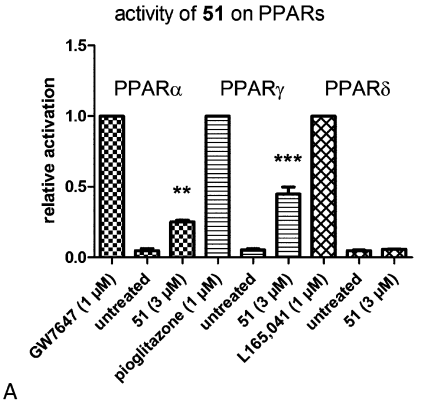

A

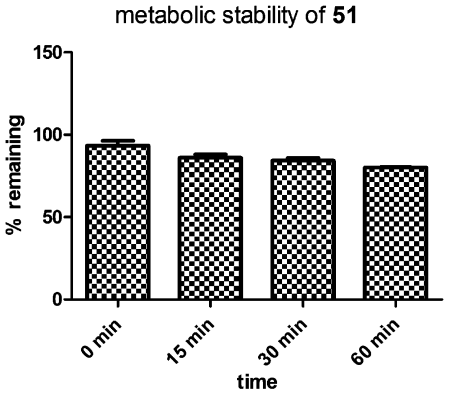

B

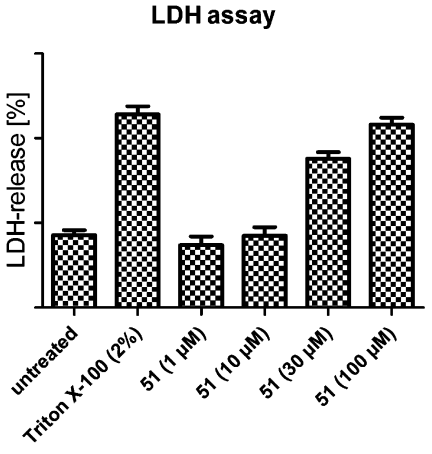

C

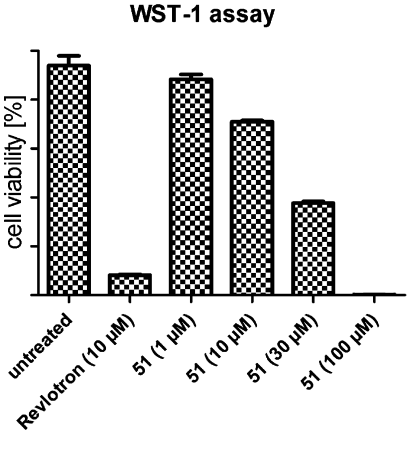

D

Figure 3. In vitro characterization of **51**. (A) off-target activity of compound **51**: **51** is highly selective over PPARs and the membrane bile acid receptor TGR5. (B) In vitro metabolism of **51** with Sprague Wistar Rat liver microsomes: after 60 min, 80.2 ± 0.2% of the compound were still detectable; $n = 4$. (C) LDH activity of HepG2 cells after 48 h treatment with compound **51**: **51** showed acute toxicity starting from 30 μM; $n = 4$. (D) WST-1 assay in HepG2 cells: 51 exhibited significant antiproliferative effects starting from 30 μM; $n = 4$.

docking poses. Accordingly, models derived from other benzimidazole-based FXR-LBD complexes led to equal results. However, docking of the anthranilic acid derivatives into models derived from FXR-LBD cocrystal structures with full agonistic ligands such as **56** revealed no reasonable docking poses in contrast. Therefore, the complex 3OLF[32] was used to generate the model for our docking studies.

Docking of lead compound **13** into the ligand binding site of FXR (model derived from PDB ID: 3OLF[32]) suggested prominent polar interactions of the benzoic acid with Arg_{335} and with Arg_{268} via a near water cluster formed by two water molecules. The lipophilic substituent was buried in a hydrophobic pocket formed by Phe_{333}, Leu_{291}, Leu_{455}, Met_{454}, and Trp_{458} (Figure 5A). Through elongation of the benzoic acid in **13** to phenylacetic acid (**31**), these interactions were weakened because the distances for polar interactions were not optimal. The Gibbs energies for the poses of **31** and **13** were however comparable (−8.9 and −8.7; Figure 5B). According to our docking, further elongation to phenylpropionic acid in **32** on the other hand strengthened the interactions with Arg_{335} and with Arg_{268} and led to displacement of one water molecule from the cluster (Figure 5C), which explains the rank order of potency of **13**, **31**, and **32**. Additionally, the Gibbs energy for the pose of **32** was significantly lower with −9.2 than for **31**.

Additionally, docking of **45** yielded an explanation for its antagonistic activity. Introduction of a chlorine substituent in 5-postion of the central aromatic ring in **45** seemed to shift the whole compound toward helix 7 and make a polar interaction with Tyr_{373} possible (Figure 5D,E). A comparable interaction of

dx.doi.org/10.1021/jm500937v | J. Med. Chem. XXXX, XXX, XXX−XXX

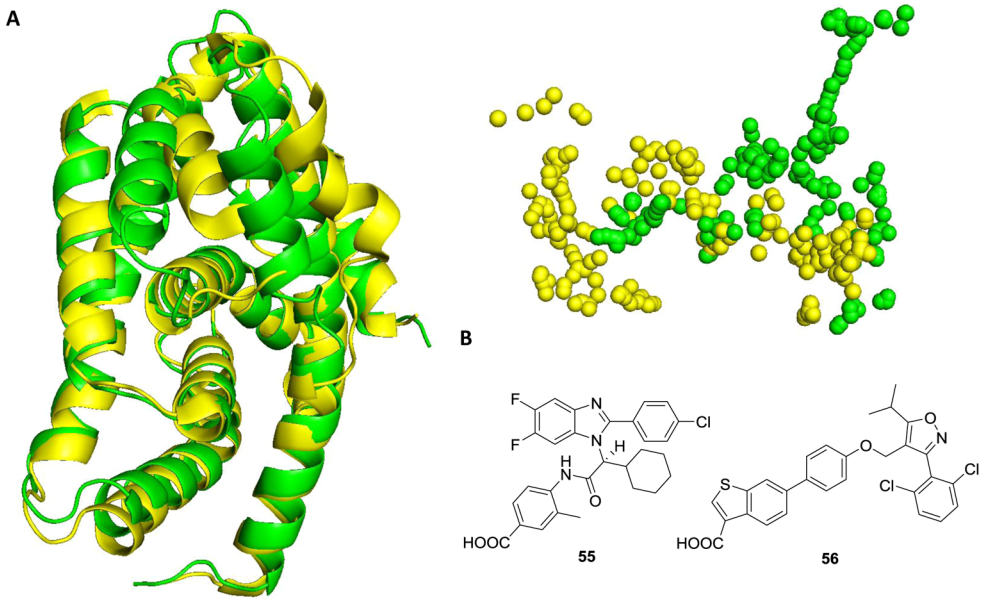

Figure 4. Comparison of the conformation (A) and pocket form (B) of the FXR-LBD cocrystal structures in complex with the partial agonist **55** (green, 3OLF) and the full agonist **56** (yellow, 3RUT). Helices 3 and 7 are shifted, which makes the ligand binding pocket of the partial agonistic conformation triangular, while in the full agonistic conformation, the pocket is long and narrow.

FXR antagonists with helix 7 has already been described previously.[33]

With an additional substituent in the 4-position of the headgroup aromatic ring (compounds **33** and **36**–**38**), the compounds cannot form the same docking pose as, e.g., **13** because the 4-substituent and the amide oxygen would form a steric clash. In the docking pose, both amide groups were flipped, and with this different geometry, a good binding pose and many beneficial interactions seemed to be lost (Figure 5F).

An additional substituent in the 4-position of the central aromatic ring (compounds **46** and **48**–**51**) in the docking was placed between helix 3 and helix 7, which slightly changed the whole binding mode of the compounds and led to a docking pose quite similar to the pose of phenylpropionic acid derivative **32**. The interactions with Arg_{335} and Arg_{268} as well as with the associated water cluster were strengthened, and one water molecule was displaced. Additionally, the docking pose suggested a further cation–π interaction of the headgroup aromatic ring with Met_{294} (Figure 5G/H). The displacement of one water molecule together with the more favorable relative position of the carboxylic acid function to Arg_{335} and Arg_{268} can explain the high rise in potency of compounds **46**, **49**, **50**, and **51**. There was no further polar interaction for compound **51**, but in addition to the displacement of one water molecule, the methoxy group and the *tert*-butylbenzoyl moiety were buried more deeply in lipophilic pockets, probably leading to the additional rise in potency (Figure 5I,J).

Substituents in the ortho-position of the carboxylic acid (6-position of headgroup, compounds **35** and **39**–**42**) also seemed to displace one water molecule from the water cluster associated with Arg_{335} and Arg_{268}, thereby increasing the potency of the compounds (Figure 5K). There seemed however not to be enough space for large substituents such as bromine (**41**) or a nitro group (**42**), which explains their loss in potency. On the other hand, the docking poses of **35** and **51** can explain why the combination of both beneficial substitutions in compounds **52** and **54** could not further improve the potency but led to approximately equally potent derivatives because one substitution alone is sufficient to displace a water from the cluster. The double substituted derivative **54** (green) was slightly twisted compared to the poses of **35** (pink) and **46** (blue). The Gibbs energies also support this thesis, with values of −9.6 for **35** and −8.3 for **53** (Figure 5K,L).

Finally, we tried to dock the optimized compound **51** in different models of the FXR-LBD derived from complexes of other compound classes than the benzimidazoles related to **55** on which our docking was based. Docking of **51** in FXR-LBD models derived from cocrystals of full FXR agonists such as **56** (PDB-ID: 3RUT[33]), which display a long and narrow binding pocket, yielded no reasonable docking poses however. The fact that **51** could only reasonably be docked in FXR models based on the partial agonistic benzimidazoles related to **55** further confirms the partial FXR agonistic activity of the acylanthranilic acid scaffold.

DISCUSSION AND CONCLUSIONS

We have intensively investigated the SAR of anthranilic acid derivatives as partial FXR agonists. Starting from compound **13**, which resulted from recombination of the best moieties in our first SAR study,[28] all structural features of the acyl anthranilamide scaffold and their impact on FXR activity have been evaluated. Inversion of the amide bonds (**14**) disrupted the activity on FXR, and we found no comparable or better lipophilic backbone substituent (compounds **15**–**22**) than the 4-*tert*-butylbenzoyl residue (**13**).

Interestingly, the acidic headgroup of **13** could be replaced by several bioisosteric moieties such as a nitrile (**24**), a methyl ketone (**23**), or even a methoxy group (**25**) without a significant change in potency. However, none of the bioisosteric groups improved the potency either and for reasons of solubility the carboxylic acid remained the most convenient residue.

By elongation of the acidic headgroup side chain from a benzoic acid (**13**) to phenylacetic acid (**31**) potency was slightly diminished, while further elongation to phenylpropionic

dx.doi.org/10.1021/jm500937v | J. Med. Chem. XXXX, XXX, XXX–XXX

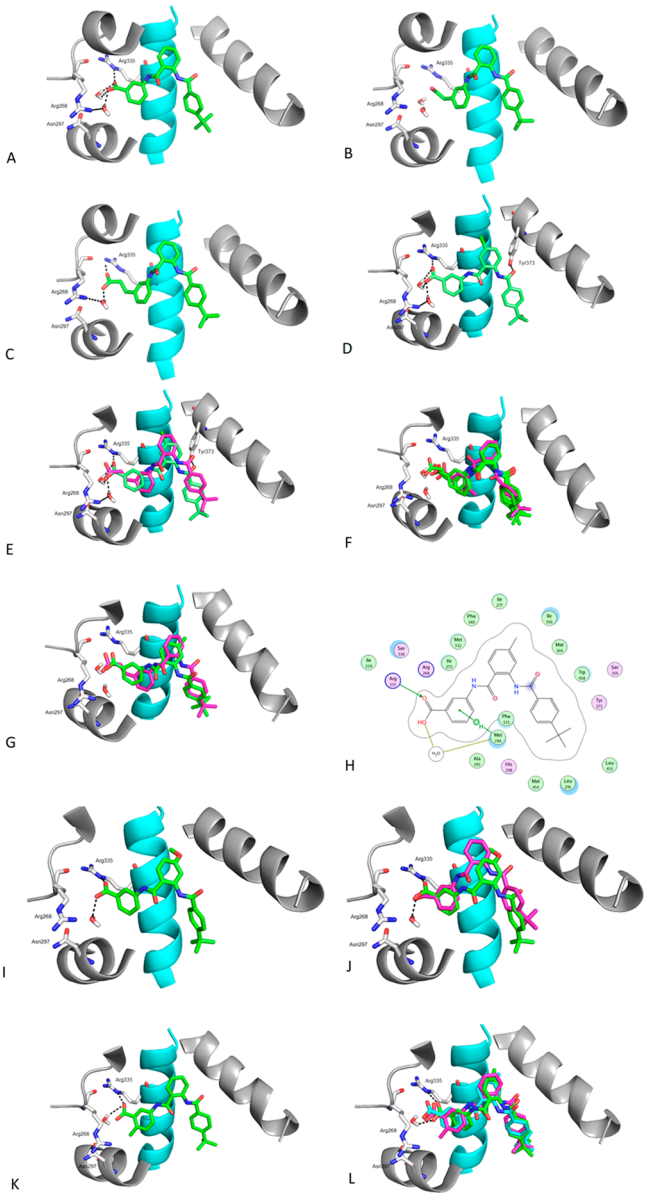

Figure 5. Docking poses of compounds docked to the FXR-LBD derived from 3OLF.[32] (A) lead compound **13**. (B) **31** with elongated side chain: the distances and angles of the acidic headgroup to Arg_{335}, Arg_{268}, and the associated water molecules are inappropriate for polar interactions. (C) **32** with further elongated side chain: **32** forms potent polar interactions with Arg_{335}, Arg_{268}, and the associated water molecules and displaces one water molecule from the cluster. (D) Antagonistic compound **45**. (E) **45** (green) in comparison with **32** (pink): **45** forms a different docking pose than the agonistic compounds and is shifted toward helix 7. (F) Introduction of an additional methyl substituent in the 4-position of the aromatic ring of the headgroup in **33** (pink) leads to a different docking pose in which the amide bonds are flipped and beneficial interactions are lost. (G) Methyl group in the 4-position of the central aromatic ring in **49** (green) leads to a docking pose similar to **32** (pink) with displacement of one water molecule from the cluster. (H) Additionally, in the docking pose, an additional interaction of **49** with Met_{294} is present. (I) Compound **51** displaces one water molecule from the water cluster and forms potent interactions with Arg_{335}, Arg_{268}, and the associated water molecule; furthermore, the lipophilic 4-*tert*-butylbenzoyl substituent is deeply buried in a lipophilic pocket and the methoxy group is placed in a lipophilic pocket next to helix 7. (J) Superimposed docking poses of **13** (pink) and **35** (green). (K) Methyl group in 6-position of the headgroup aromatic ring (**35**) also seems to displace one water molecule and forms a similar docking pose as **32** and **51**. (L) Superimposed docking poses of **35** (pink), **49** (light blue), and **54** (green): introduction of two methyl groups (4-position of the central aromatic ring and 6-position of the headgroup aromatic ring) does not lead to a more beneficial docking pose because each methyl group alone is sufficient to displace one water from the cluster associated with Arg_{335} and Arg_{268}.

acid (**32**) strongly improved the potency. This rank order of potency is best explained by interaction of the headgroup with a water cluster associated with Arg_{335} and Arg_{268} as suggested by the docking pose. While the benzoic acid (**13**) can well interact with the water cluster, for the phenylacetic acid moiety (**31**), angles and distances might be inappropriate for good interaction, and finally, the phenylpropionic acid (**32**) seems to form potent interactions with Arg_{335} and Arg_{268} and to displace one water molecule from the cluster.

By selectively substituting all free positions of the headgroup (**33**−**42**) and central aromatic ring (**43**−**51**), we discovered positions that through substitution either disrupted the activity of the compounds on FXR or strongly improved their potency. Additional substituents on the central aromatic moiety next to the amide bonds (**43** and **44**) led to inactivity which is probably due to steric clashes with the amide bonds and a consequently different geometry of the compounds. Substituents in the 4-position of the headgroup aromatic ring (**33**, **36**−**38**) strongly reduced the potency as well. The fact that a fluorine atom, which constitutes the smallest substituent in this series, retained most activity indicates that the loss of potency is as well due to steric interactions with the amide group in proximity.

Substituents in the 4-position of the central aromatic ring (**46**, **49**−**51**) and in the 6-position of the headgroup (**35**, **39**−**41**) both strongly improved the potency of the compounds. In the case of the headgroup, the SAR was quite steep because only a methyl (**35**) and a methoxy group (**39**) were highly potent while larger substituents were less active. Our docking studies suggest that the gain in potency of **35** and **39** might be due to displacement of one water molecule from the water cluster associated with Arg_{335} and Arg_{268}.

Furthermore, in the case of 5-substituted derivatives (**45** and **47**) of the central aromatic ring, we found two FXR antagonists. According to our docking studies, the additional substituent seems to change slightly the binding mode of the whole scaffold and make a polar interaction of the *tert*-butylbenzoylamide oxygen with Tyr_{373} in helix 7 possible. It has been suggested[34] that interaction with helix 7 might lead to antagonistic activity on FXR, which here seems to be true as well.

The strongest improvement in agonistic activity was gained by introduction of substituents in the 4-position of the central aromatic ring. A methyl group (**49**), a chlorine atom (**46**), and a bromine atom (**50**) in this position led to equally potent derivatives, which is according to our docking studies due to a slight shift in the binding mode toward Arg_{335} and Arg_{268} and the associated water cluster. The docking pose of **49** is similar to the pose of phenylpropionic acid derivative **32** and reveals better angles and distances for polar interactions with Arg_{335} and Arg_{268} as well as displacement of one water molecule. A methoxy group (**51**) in the 4-position of the central aromatic ring showed even more potency on FXR and a very favorable docking pose.

dx.doi.org/10.1021/jm500937v | *J. Med. Chem.* XXXX, XXX, XXX−XXX

The resulting compound **51** of this SAR study constitutes a highly potent and selective partial FXR agonist (EC_{50} = 8 ± 3 nM, 17.5 ± 0.7% max) with good physicochemical properties, acceptable solubility, high metabolic stability, and acceptable toxicity compared to its potency. The fact that the effect of **51** on FXR target genes was not concentration dependent in the investigated range from 0.1 to 10 μM shows that **51** exhibits true partial FXR agonism which might be of therapeutic value for metabolic disorders because full activation of nuclear receptors over long-term treatment has been observed to cause negative effects as well, e.g., for full FXR agonists, promoting effects on proliferation and migration of several forms of cancer have been observed[35−40] and FXR agonism might induce impaired cholesterol homeostasis[41] because the conversion of cholesterol to bile acids and their elimination are inhibited by FXR activation. Overactivation of the nuclear receptor might also evoke a cholestatic condition,[2] and finally FXR agonism can cause serious liver damage in cholestasis.[42] The development of FXR targeting drugs therefore must either find the right balance between beneficial FXR activation and disadvantageous overactivation or discover target gene selective FXR modulators that similarly to the selective estrogen-receptor modulators (SERMs) exhibit differential effects on different target genes. The here reported highly potent FXR partial agonist **51** constitutes a novel FXR targeting agent that only moderately activates the nuclear receptor and might display one possible way to overcome the handicaps of full FXR agonists.

EXPERIMENTAL SECTION

General. All chemicals and solvents were of reagent grade and used without further purification unless otherwise specified. ^{1}H NMR and ^{13}C NMR spectra were measured in DMSO-d_6 on a Bruker AV 500, Bruker AV 400, Bruker AV 300, or Bruker am250xp spectrometer. Chemical shifts are reported in parts per million (ppm), with tetramethylsilane (TMS) as an internal standard. Mass spectra were obtained on a Fisons Instruments VG Plattform II measuring in the positive- or negative-ion mode (ESI−MS system). The purity of the final compounds was determined by combustion analysis, which was performed by the Microanalytical Laboratory of the Institute of Organic Chemistry and Chemical Biology, Goethe University Frankfurt, on an Elementar Vario Micro Cube. All tested compounds described here have a purity ≥95%. Intermediates were not analyzed.

Synthesis. General Procedures. *a. ortho-Aminobenzoylation with Isatoic Anhydride Derivatives.* Isatoic anhydride derivative (**5a−f**, 1.0 equiv) and 4-*N*,*N*-dimethylaminopyridine (0.1 equiv) were dissolved in a mixture of pyridine (2 mL/mmol **5a−f**) and DMF (0.5 mL/mmol **4a**,**b**) and heated to 80 °C. After a clear brown solution had formed, the respective aniline derivative (**4a−u**, 1.1 equiv) was added in one portion. With addition of NEt_3 (0.5 mL/mmol **5a−f**), the formation of carbon dioxide started. The reaction mixture was kept at 80 °C for 16 h. Then the solvents were evaporated in vacuum and the crude product dissolved in ethyl acetate. The organic phase was washed twice with 10% hydrochloric acid and brine and dried over Na_2SO_4. Further purification was performed by recrystallization or column chromatography on silica.

Aniline derivative (**4a−u**, 1.0 equiv) was dissolved in EtOH (abs, 5 mL/mmol **4a−u**) and heated to reflux. When the mixture had cleared and reached at least 80 °C, isatoic anhydride derivative (**5a−f**, 2.0 equiv) was added in one portion with the immediate formation of carbon dioxide. The reaction mixture was stirred under reflux for 60 min. After cooling to room temperature, volume was reduced in vacuum until crystallization of the product initiated and the crude product was filtered off. When no crystallization was possible, the crude product was partitioned between ethyl acetate and 10% hydrochloric acid, the aqueous layer was extracted with additional ethyl acetate three times, the combined organic layers were dried over Na_2SO_4, and solvent was evaporated in vacuum. The crude product was further purified by recrystallization or column chromatography on silica.

b. ortho-Nitrobenzoylation with Benzoic Acid Derivatives. *ortho*-Nitrobenzoic acid derivative (**6a−f**, 1.0 equiv) was dissolved in CH_2Cl_2 (abs, 5 mL/mmol **6a−f**) and DMF (abs, 0.1 mL/mmol **6a−f**). Thionyl chloride (1.3 equiv) was added slowly at room temperature, and the mixture was stirred 4 h under reflux. Solvents were evaporated in vacuum, and the crude product (**9a−f**) was dried in ultravacuum. Without further purification the crude product (**9a−f**) was used for reaction with aniline derivatives (**4a−u**): for this purpose aniline derivative (**4a−u**, 1.3 equiv) was dissolved in CH_2Cl_2 (abs, 5 mL/mmol **6a−f**) and pyridine (abs, 1 mL/mmol **6a−f**), and the crude *ortho*-nitrobenzoyl chloride derivative (**9a−f**) in CH_2Cl_2 (abs, 5 mL/mmol **6a−f**) was added dropwise. The mixture was stirred at room temperature until TLC indicated consumption of starting material (4−12 h). The reaction mixture was then poured into an equal volume 10% hydrochloric acid, phases were separated, and the aqueous phase was extracted three times with ethyl acetate. Combined organic layers were dried over Na_2SO_4, and solvent was evaporated in vacuum. Further purification was performed by recrystallization or column chromatography on silica.

c. Reduction of ortho-Nitrobenzoylaniline Derivatives. *ortho*-Nitrobenzoylaniline derivative (**10a−e**, 1.0 equiv) was dissolved in THF (abs, 10 mL/mmol), tin (3.5 equiv) was added, and the mixture was heated to 50 °C. Hydrochloric acid (36%, 7 equiv) was added slowly, and the mixture was stirred under reflux for 60 min, then filtered, diluted with an equal volume ethyl acetate, and washed twice with water. The combined aqueous layers were extracted three times with ethyl acetate, and the combined organic layers were dried over Na_2SO_4 and solvent was evaporated in vacuum. Further purification was performed by recrystallization or column chromatography on silica.

d. Acylation of Anthranilic Acid Derivatives. Anthranilic acid derivative (**7a−z**, **10a−e**, 1.0 equiv) was dissolved in THF (3 mL/mmol **7a−z**, **10a−e**), and pyridine (3.0 equiv) was added. After a clear solution had formed, the respective acyl chloride (**8a−j**, 1.3 equiv) was added in THF (2 mL/mmol **7a−z**, **10a−e**). The reaction mixture was kept at room temperature for 4−8 h, and the reaction progress was monitored by TLC. When anthranilic acid derivative (**7a−z**, **10a−e**) was consumed, the reaction mixture was diluted with ethyl acetate and washed three times with 10% hydrochloric acid, and dried over Na_2SO_4. Further purification was performed by column chromatography on silica and recrystallization.

e. Alkaline Ester Hydrolysis. The respective ester was dissolved in THF (9 mL/mmol), and aqueous LiOH solution (10%, 1 mL/mmol) was added slowly. The mixture was then stirred at room temperature or at 40 °C until TLC indicated complete conversion of the starting material (12−24 h). The mixture was then poured into 10% aqueous hydrochloric acid, an equal volume of ethyl acetate was added, and phases were separated. The aqueous layer was extracted three times with ethyl acetate, the combined organic layers were dried over Na_2SO_4, and solvent was evaporated in vacuum. Further purification was performed by recrystallization or column chromatography on silica.

Test Compounds. *3-(2-(4-(tert-Butyl)benzamido)benzamido)-benzoic Acid (**13**).* Preparation according to general procedure d using **7a** and *tert*-butylbenzoyl chloride (**8a**). After column chromatography on silica with hexane/ethyl acetate/acetic acid (89:9:2) as mobile phase, the product was recrystallized from hexane/ethyl acetate to give **13** as white solid in 77% yield. R_f (hexane/ethyl acetate/acetic acid (49:49:2)) = 0.58. ^{1}H NMR (500 MHz, DMSO) δ = 13.03 (s, 1H), 11.55 (s, 1H), 10.70 (s, 1H), 8.32 (t, J = 1.8 Hz, 1H), 8.00−7.96 (m, 1H), 7.95 (dd, J = 7.9, 1.2 Hz, 1H), 7.87−7.84 (m, 1H), 7.78 (d, J = 8.5 Hz, 1H), 7.74−7.71 (m, 1H), 7.59 (d, J = 8.5 Hz, 2H), 7.51 (t, J = 7.9 Hz, 1H), 7.48−7.45 (m, 1H), 7.32−7.28 (m, 2H), 1.31 (s, 9H). ^{13}C NMR (126 MHz, DMSO) δ = 168.08, 167.58, 165.08, 155.48, 139.26, 132.83, 132.23, 131.72, 129.56, 129.43, 127.39, 126.21, 126.04, 125.69, 125.47, 123.69, 123.20, 122.32, 121.79, 35.22, 31.34. $C_{25}H_{24}N_2O_4$. MS (ESI−): m/z 415.9 ([M − HM

dx.doi.org/10.1021/jm500937v | J. Med. Chem. XXXX, XXX, XXX−XXX

− H]⁻, 100). Combustion analysis measured (calculated): C 72.17 (72.10); H 6.21 (5.81); N 6.64 (6.73).

*3-((2-((4-(tert-Butyl)phenyl)carbamoyl)phenyl)carbamoyl)-benzoic Acid (**14**).* Preparation according to general procedure e using **14a**. After column chromatography on silica with hexane/ethyl acetate/acetic acid (89:9:2) as mobile phase, the product was recrystallized from hexane/ethyl acetate to give **14** as white solid in 89% yield. R_f (hexane/ethyl acetate/acetic acid (49:49:2)) = 0.60. ^{1}H NMR (500 MHz, DMSO) δ = 13.32 (s, 1H), 11.81 (s, 1H), 10.50 (s, 1H), 8.52 (s, 1H), 8.42 (d, J = 8.1 Hz, 1H), 8.15 (dd, J = 14.2, 7.8 Hz, 2H), 7.92 (d, J = 7.6 Hz, 1H), 7.72 (t, J = 7.7 Hz, 1H), 7.63 (t, J = 7.2 Hz, 3H), 7.38 (d, J = 8.6 Hz, 2H), 7.32 (t, J = 7.5 Hz, 1H), 1.28 (s, 9H). ^{13}C NMR (126 MHz, DMSO) δ = 167.64, 167.10, 164.32, 147.11, 138.76, 136.37, 135.32, 133.02, 132.58, 131.93, 131.55, 129.87, 129.36, 128.55, 125.75, 124.05, 123.98, 122.10, 121.33, 34.58, 31.65. $C_{25}H_{24}N_2O_4$. MS (ESI−): m/z 415.26 ([M − H]⁻, 100), 451.24 ([M + Cl]⁻, 46). Combustion analysis measured (calculated): C 72.01 (72.10); H 6.18 (5.81); N 6.72 (6.73).

*2-Methyl-5-(2-(4-(trifluoromethyl)benzamido)benzamido)-benzoic Acid (**15**).* Preparation according to general procedure d using **7a** and 4-(trifluoromethyl)benzoyl chloride (**8b**). After column chromatography on silica with hexane/ethyl acetate/acetic acid (89:9:2) as mobile phase, the product was recrystallized from hexane/ethyl acetate to give **15** as white solid in 78% yield. R_f (hexane/ethyl acetate/acetic acid (49:49:2)) = 0.54. ^{1}H NMR (500 MHz, DMSO) δ = 13.00 (s, 1H), 11.56 (s, 1H), 10.70 (s, 1H), 8.34−8.30 (m, 2H), 8.11 (d, J = 8.2 Hz, 2H), 7.95 (dd, J = 11.5, 8.2 Hz, 4H), 7.71 (d, J = 7.7 Hz, 1H), 7.67−7.62 (m, 1H), 7.49 (t, J = 7.9 Hz, 1H), 7.35 (dd, J = 11.1, 4.1 Hz, 1H). ^{13}C NMR (126 MHz, DMSO) δ = 167.75, 167.60, 164.18, 139.36, 138.83, 138.30, 132.63, 132.28, 132.03, 131.79, 129.57, 129.38, 128.57, 126.38, 126.35, 125.50, 125.37, 124.82, 124.46, 123.23, 122.63, 122.18, 21.54. $C_{23}H_{17}F_3N_2O_4$. MS (ESI−): m/z 427.8 ([M − H]⁻, 100). Combustion analysis measured (calculated): C 61.32 (61.69); H 3.58 (3.53); N 6.48 (6.54).

*3-(2-(4-Bromobenzamido)benzamido)benzoic Acid (**16**).* Preparation according to general procedure d using **7a** and 4-bromobenzoyl chloride (**8c**). After column chromatography on silica with hexane/ethyl acetate/acetic acid (89:9:2) as mobile phase, the product was recrystallized from hexane/ethyl acetate to give **16** as white solid in 30% yield. R_f (hexane/ethyl acetate/acetic acid (49:49:2)) = 0.51. ^{1}H NMR (500 MHz, DMSO) δ = 11.48 (s, 1H), 10.69 (s, 1H), 8.33 (d, J = 8.3 Hz, 1H), 8.32 (s, 1H), 7.96 (d, J = 8.1 Hz, 1H), 7.94−7.91 (m, 1H), 7.87−7.82 (m, 2H), 7.79 (d, J = 8.6 Hz, 2H), 7.71 (d, J = 7.8 Hz, 1H), 7.66−7.60 (m, 1H), 7.49 (t, J = 7.9 Hz, 1H), 7.32 (dd, J = 11.0, 4.2 Hz, 1H). ^{13}C NMR (126 MHz, DMSO) δ = 168.64, 167.84, 167.58, 164.38, 139.32, 138.56, 134.12, 132.66, 132.37, 129.68, 129.55, 129.39, 126.27, 125.55, 125.39, 124.36, 124.19, 122.41, 122.21. $C_{21}H_{15}BrN_2O_4$. MS (ESI+): m/z 461.29 ([M + Na]⁺, 95); 463.29 ([M + Na]⁺, 100). Combustion analysis measured (calculated): C 57.21 (57.42); H 3.70 (3.44); N 6.19 (6.38).

*3-(2-(Benzo[d][1,3]dioxole-5-carboxamido)benzamido)benzoic Acid (**17**).* Preparation according to general procedure d using **7a** and benzo[*d*][1,3]dioxole-5-carbonyl chloride (**8d**). After column chromatography on silica with hexane/ethyl acetate/acetic acid (89:9:2) as mobile phase, the product was recrystallized from hexane/ethyl acetate to give **17** as white solid in 45% yield. R_f (hexane/ethyl acetate/acetic acid (49:49:2)) = 0.41. ^{1}H NMR (500 MHz, DMSO) δ = 13.03 (s, 1H), 11.40 (s, 1H), 10.69 (s, 1H), 8.40 (d, J = 7.6 Hz, 1H), 8.33 (t, J = 1.8 Hz, 1H), 7.97 (dd, J = 8.1, 1.1 Hz, 1H), 7.93 (dd, J = 7.9, 1.1 Hz, 1H), 7.74−7.70 (m, 1H), 7.64−7.59 (m, 1H), 7.53−7.47 (m, 2H), 7.40 (d, J = 1.7 Hz, 1H), 7.29 (td, J = 7.8, 1.0 Hz, 1H), 7.09 (d, J = 8.1 Hz, 1H), 6.14 (s, 2H). ^{13}C NMR (126 MHz, DMSO) δ = 168.01, 167.58, 164.37, 150.91, 148.23, 139.31, 139.07, 132.74, 131.71, 129.54, 129.42, 128.97, 125.60, 125.42, 123.73, 123.58, 122.63, 122.22, 122.01, 108.81, 107.62, 102.45. $C_{22}H_{16}N_2O_6$. MS (ESI+): m/z 405.37 ([M + H]⁺, 23), 427.37 ([M + Na]⁺, 100). Combustion analysis measured (calculated): C 64.96 (65.35); H 4.28 (3.99); N 6.77 (6.93).

*3-(2-(2,3-Dihydrobenzo[b][1,4]dioxine-6-carboxamido)-benzamido)benzoic Acid (**18**).* Preparation according to general procedure d using **7a** and 2,3-dihydrobenzo[*b*][1,4]dioxine-6-carbonyl chloride (**8e**). After column chromatography on silica with hexane/ethyl acetate/acetic acid (89:9:2) as mobile phase, the product was recrystallized from hexane/ethyl acetate to give **18** as white solid in 41% yield. R_f (hexane/ethyl acetate/acetic acid (49:49:2)) = 0.34. ^{1}H NMR (500 MHz, DMSO) δ = 13.04 (s, 1H), 11.44 (s, 1H), 10.69 (s, 1H), 8.42 (d, J = 7.7 Hz, 1H), 8.32 (s, 1H), 7.97 (dd, J = 8.1, 1.0 Hz, 1H), 7.95−7.91 (m, 1H), 7.72 (d, J = 7.8 Hz, 1H), 7.64−7.59 (m, 1H), 7.51 (t, J = 7.9 Hz, 1H), 7.44−7.39 (m, 2H), 7.31−7.26 (m, 1H), 7.03 (d, J = 8.4 Hz, 1H), 4.31 (dd, J = 10.7, 5.1 Hz, 4H). ^{13}C NMR (126 MHz, DMSO) δ = 168.07, 167.57, 164.32, 147.24, 143.73, 139.27, 139.18, 132.78, 131.73, 129.55, 129.43, 127.87, 125.66, 125.45, 123.63, 123.27, 122.29, 121.85, 120.94, 117.85, 116.59, 64.86, 64.48. $C_{23}H_{18}N_2O_6$. MS (ESI+): m/z 419.37 ([M + H]⁺, 16), 441.37 ([M + Na]⁺, 100). Combustion analysis measured (calculated): C 65.57 (66.03); H 4.62 (4.34); N 6.93 (6.70).

*3-(2-(3-Fluoro-4-(trifluoromethyl)benzamido)benzamido)-benzoic Acid (**19**).* Preparation according to general procedure d using **7a** and 3-fluoro-4-(trifluoromethyl)benzoyl chloride (**8f**). After column chromatography on silica with hexane/ethyl acetate/acetic acid (89:9:2) as mobile phase, the product was recrystallized from hexane/ethyl acetate to give **19** as white solid in 73% yield. R_f (hexane/ethyl acetate/acetic acid (49:49:2)) = 0.53. ^{1}H NMR (500 MHz, DMSO) δ = 13.01 (s, 1H), 11.46 (s, 1H), 10.69 (s, 1H), 8.34 (s, 1H), 8.21 (d, J = 8.2 Hz, 1H), 8.03 (t, J = 7.7 Hz, 1H), 7.95 (d, J = 10.2 Hz, 2H), 7.91 (d, J = 8.0 Hz, 2H), 7.70 (d, J = 7.6 Hz, 1H), 7.65 (t, J = 7.8 Hz, 1H), 7.48 (t, J = 7.9 Hz, 1H), 7.37 (t, J = 7.5 Hz, 1H). ^{13}C NMR (126 MHz, DMSO) δ = 167.60, 167.52, 163.00, 141.73, 139.45, 137.72, 132.49, 131.74, 129.58, 129.37, 128.78, 125.76, 125.37, 125.30, 124.86, 124.16, 124.13, 123.11, 122.04, 121.67, 116.65, 116.47. $C_{22}H_{14}F_4N_2O_4$. MS (ESI+): m/z 469.38 ([M + Na]⁺, 100). Combustion analysis measured (calculated): C 58.97 (59.20); H 3.17 (3.16); N 6.38 (6.28).

*3-(2-(3,5-Bis(trifluoromethyl)benzamido)benzamido)benzoic Acid (**20**).* Preparation according to general procedure d using **7a** and 3,5-bis(trifluoromethyl)benzoyl chloride (**8g**). After column chromatography on silica with hexane/ethyl acetate/acetic acid (89:9:2) as mobile phase, the product was recrystallized from hexane/ethyl acetate to give **20** as white solid in 66% yield. R_f (hexane/ethyl acetate/acetic acid (49:49:2)) = 0.57. ^{1}H NMR (500 MHz, DMSO) δ = 12.95 (s, 1H), 11.33 (s, 1H), 10.63 (s, 1H), 8.50 (s, 2H), 8.38 (s, 2H), 7.98 (d, J = 8.1 Hz, 1H), 7.94 (d, J = 8.0 Hz, 1H), 7.85 (d, J = 7.1 Hz, 1H), 7.68−7.65 (m, 1H), 7.65−7.62 (m, 1H), 7.44 (t, J = 7.9 Hz, 1H), 7.39 (td, J = 7.7, 0.9 Hz, 1H). ^{13}C NMR (126 MHz, DMSO) δ = 167.59, 167.11, 162.91, 139.70, 137.43, 136.83, 132.07, 131.69, 131.29, 131.02, 129.53, 129.24, 128.69, 125.87, 125.38, 125.04, 124.83, 124.57, 124.22, 121.58. $C_{23}H_{14}F_6N_2O_4$. MS (ESI+): m/z 519.4 ([M + Na]⁺, 100). Combustion analysis measured (calculated): C 55.55 (55.66); H 2.76 (2.84); N 5.63 (5.64).

*3-(2-(2-Phenylacetamido)benzamido)benzoic Acid (**21**).* Preparation according to general procedure d using **7a** and phenylacetyl chloride (**8h**). After column chromatography on silica with hexane/ethyl acetate/acetic acid (89:9:2) as mobile phase, the product was recrystallized from hexane/ethyl acetate to give **21** as white solid in 72% yield. R_f (hexane/ethyl acetate/acetic acid (49:49:2)) = 0.43. ^{1}H NMR (500 MHz, DMSO) δ = 13.02 (s, 1H), 10.56 (s, 1H), 10.45 (s, 1H), 8.40 (s, 1H), 8.11 (d, J = 8.3 Hz, 1H), 7.90 (t, J = 14.3 Hz, 1H), 7.77 (d, J = 7.7 Hz, 1H), 7.71 (d, J = 7.7 Hz, 1H), 7.51 (dt, J = 12.8, 7.7 Hz, 2H), 7.36−7.26 (m, 4H), 7.26−7.21 (m, 2H), 3.70 (s, 2H). ^{13}C NMR (126 MHz, DMSO) δ = 169.75, 167.68, 167.30, 139.56, 137.91, 135.79, 132.07, 131.68, 129.83, 129.30, 129.09, 128.85, 127.16, 125.34, 125.18, 125.11, 123.87, 122.45, 121.77, 44.20. $C_{22}H_{18}N_2O_4$. MS (ESI+): m/z 375.38 ([M + H]⁺, 20), 397.36 ([M + Na]⁺, 100). Combustion analysis measured (calculated): C 70.50 (70.58); H 4.97 (4.85); N 7.43 (7.48).

*3-(2-Cinnamamidobenzamido)benzoic Acid (**22**).* Preparation according to general procedure d using **7a** and cinnamoyl chloride (**8i**). After column chromatography on silica with hexane/ethyl acetate/acetic acid (89:9:2) as mobile phase, the product was recrystallized from hexane/ethyl acetate to give **22** as white solid in 42% yield. R_f (hexane/ethyl acetate/acetic acid (49:49:2)) = 0.48. ^{1}H

dx.doi.org/10.1021/jm500937v | J. Med. Chem. XXXX, XXX, XXX−XXX

NMR (500 MHz, DMSO) δ = 13.02 (s, 1H), 10.66 (d, J = 12.5 Hz, 1H), 10.59 (s, 1H), 8.42 (s, 1H), 8.28 (d, J = 8.2 Hz, 1H), 8.01−7.92 (m, 1H), 7.82 (dd, J = 7.7, 1.0 Hz, 1H), 7.74−7.66 (m, 3H), 7.62−7.55 (m, 2H), 7.49 (t, J = 7.9 Hz, 1H), 7.46−7.38 (m, 3H), 7.31−7.25 (m, 1H), 6.93 (d, J = 15.7 Hz, 1H). ^{13}C NMR (126 MHz, DMSO) δ = 167.64, 167.46, 164.14, 141.44, 139.61, 138.11, 135.01, 132.17, 131.70, 130.37, 129.39, 129.33, 128.54, 125.24, 125.21, 123.93, 122.75, 122.65, 121.88. $C_{23}H_{18}N_2O_4$. MS (ESI−): m/z 485.24 ([M − H]$^-$, 100). Combustion analysis measured (calculated): C 71.11 (71.49); H 4.75 (4.70); N 7.32 (7.25).

N-(3-Acetylphenyl)-2-(4-(tert-butyl)benzamido)benzamide (**23**). Preparation according to general procedure d using **7b** and *tert*-butylbenzoyl chloride (**8a**). After column chromatography on silica with hexane/ethyl acetate/acetic acid (89:9:2) as mobile phase, the product was recrystallized from hexane/ethyl acetate to give **23** as white solid in 27% yield. R_f (hexane/ethyl acetate (4:1)) = 0.63. ^{1}H NMR (500 MHz, DMSO) δ = 11.59 (s, 1H), 10.72 (s, 1H), 8.48 (dd, J = 8.3, 0.8 Hz, 1H), 8.26 (t, J = 1.8 Hz, 1H), 8.03 (dd, J = 8.1, 1.2 Hz, 1H), 7.95 (dt, J = 14.9, 7.5 Hz, 1H), 7.90−7.82 (m, 2H), 7.79−7.74 (m, 1H), 7.67−7.60 (m, 1H), 7.60−7.57 (m, 2H), 7.55 (dd, J = 10.0, 5.9 Hz, 1H), 7.30 (td, J = 7.7, 1.1 Hz, 1H), 2.59 (s, 3H), 1.31 (s, 9H). ^{13}C NMR (126 MHz, DMSO) δ = 198.08, 168.12, 165.06, 155.47, 139.39, 139.25, 137.73, 132.87, 132.21, 129.59, 129.51, 127.40, 126.19, 126.10, 124.73, 123.67, 123.10, 121.79, 120.88, 35.21, 31.33, 27.25. $C_{26}H_{26}N_2O_3$. MS (ESI−): m/z 413.25 ([M − H]$^-$, 100). Combustion analysis measured (calculated): C 75.16 (75.34); H 6.32 (6.32); N 6.56 (6.76).

2-(4-(tert-Butyl)benzamido)-N-(3-cyanophenyl)benzamide (**24**). Preparation according to general procedure d using **7c** and *tert*-butylbenzoyl chloride (**8a**). After column chromatography on silica with hexane/ethyl acetate/acetic acid (89:9:2) as mobile phase, the product was recrystallized from hexane/ethyl acetate to give **24** as white solid in 59% yield. R_f (hexane/ethyl acetate/acetic acid (49:49:2)) = 0.74. ^{1}H NMR (500 MHz, DMSO) δ = 11.38 (s, 1H), 10.80 (s, 1H), 8.40 (dd, J = 11.6, 3.9 Hz, 1H), 8.16 (s, 1H), 8.04−7.97 (m, 1H), 7.91 (dd, J = 7.8, 1.3 Hz, 1H), 7.88−7.83 (m, 2H), 7.66−7.62 (m, 1H), 7.62−7.58 (m, 4H), 7.32 (td, J = 7.7, 1.0 Hz, 1H), 1.32 (s, 9H). ^{13}C NMR (126 MHz, DMSO) δ = 168.17, 165.15, 155.48, 140.01, 139.00, 132.93, 132.16, 130.66, 129.53, 128.09, 127.46, 126.18, 125.99, 124.11, 123.85, 123.60, 122.14, 119.17, 111.94, 35.22, 31.35. $C_{25}H_{23}N_3O_2$. MS (ESI−): m/z 396.7 ([M − H]$^-$, 100). HRMS (MALDI+) measured for [M + K]$^+$ (calculated): 436.14240 (436.14219). HPLC purity 100% (H_2O/MeOH gradient, 25 min).

2-(4-(tert-Butyl)benzamido)-N-(3-methoxyphenyl)benzamide (**25**). Preparation according to general procedure d using **7d** and *tert*-butylbenzoyl chloride (**8a**). After column chromatography on silica with hexane/ethyl acetate/acetic acid (89:9:2) as mobile phase, the product was recrystallized from hexane/ethyl acetate to give **25** as white solid in 52% yield. R_f (hexane/ethyl acetate/acetic acid (39:9:2)) = 0.35. ^{1}H NMR (500 MHz, DMSO) δ = 11.67 (s, 1H), 10.50 (s, 1H), 8.52 (s, 1H), 7.92 (d, J = 7.8 Hz, 1H), 7.86 (d, J = 8.3 Hz, 2H), 7.65−7.57 (m, 3H), 7.35 (d, J = 8.4 Hz, 2H), 7.29 (t, J = 7.6 Hz, 2H), 6.76−6.72 (m, 1H), 3.76 (s, 3H), 1.30 (d, J = 8.5 Hz, 9H). ^{13}C NMR (126 MHz, DMSO) δ = 167.97, 164.97, 159.87, 155.49, 140.10, 139.28, 132.76, 132.18, 129.94, 129.46, 127.35, 126.22, 123.58, 123.03, 121.60, 113.86, 109.99, 107.56, 55.53, 35.21, 31.33. $C_{25}H_{26}N_2O_3$. MS (ESI−): m/z 401.14 ([M − H]$^-$, 100). Combustion analysis measured (calculated): C 74.41 (74.60); H 6.56 (6.51); N 6.83 (6.96).

2-(4-(tert-Butyl)benzamido)-N-(3-(methylthio)phenyl)benzamide (**26**). Preparation according to general procedure d using **7e** and *tert*-butylbenzoyl chloride (**8a**). After column chromatography on silica with hexane/ethyl acetate/acetic acid (89:9:2) as mobile phase, the product was recrystallized from hexane/ethyl acetate to give **26** as white solid in 58% yield. R_f (hexane/ethyl acetate/acetic acid (49:49:2)) = 0.79. ^{1}H NMR (500 MHz, DMSO) δ = 11.58 (s, 1H), 10.53 (s, 1H), 8.48 (d, J = 8.2 Hz, 1H), 7.94−7.89 (m, 1H), 7.86 (t, J = 7.6 Hz, 2H), 7.66−7.58 (m, 4H), 7.55 (d, J = 8.1 Hz, 1H), 7.34−7.27 (m, 2H), 7.05 (dd, J = 7.9, 0.9 Hz, 1H), 2.48 (s, 3H), 1.31 (s, 9H). ^{13}C NMR (126 MHz, DMSO) δ = 167.98, 165.02, 155.49, 139.52, 139.18, 138.97, 132.78, 132.20, 129.66, 129.47, 127.39, 126.22, 123.66, 123.25, 122.07, 121.74, 118.67, 118.06, 35.22, 31.35, 15.12. $C_{25}H_{26}N_2O_2S$. MS (ESI+): m/z 419.46 ([M + H]$^+$, 15); 441.44 ([M + Na]$^+$, 100). Combustion analysis measured (calculated): C 71.78 (71.74); H 5.96 (6.26); N 6.79 (6.69); S 7.33 (7.66).

N-(3-(1H-Tetrazol-5-yl)phenyl)-2-(4-(tert-butyl)benzamido)-benzamide (**27**). **24** (199 mg, 0.5 mmol, 1.0 equiv) was dissolved in 5 mL of DMF/MeOH (9:1), and Cu_2O (3.6 mg, 5 mol %) and NaN_3 (297 mg, 3.0 mmol, 6.0 equiv) were added. The mixture was stirred at 90 °C for 24 h. After cooling to room temperature, 15 mL of 5% aqueous hydrochloric acid and 10 mL of CH_2Cl_2 were added and the mixture was vigorously stirred for another 30 min. Phases were then separated, and the aqueous phase was extracted with equal volumes of ethyl acetate three times. The combined aqueous layers were dried over Na_2SO_4, and the solvents were evaporated in vacuum. Further purification was performed by column chromatography on silica with hexane/ethyl acetate/acetic acid and recrystallization from acetone/water to obtain **27** as white solid in 20% yield. R_f (hexane/ethyl acetate/acetic acid (49:49:2)) = 0.15. ^{1}H NMR (500 MHz, DMSO) δ = 11.53 (s, 1H), 10.79 (s, 1H), 8.49 (t, J = 1.8 Hz, 1H), 8.46 (dd, J = 8.3, 0.9 Hz, 1H), 7.97 (dd, J = 7.9, 1.3 Hz, 1H), 7.93−7.89 (m, 1H), 7.88−7.84 (m, 2H), 7.79 (d, J = 7.8 Hz, 1H), 7.67−7.57 (m, 4H), 7.32 (td, J = 7.7, 1.1 Hz, 1H), 1.31 (s, 9H). ^{13}C NMR (126 MHz, DMSO) δ = 192.78, 168.15, 165.11, 155.48, 139.97, 139.17, 132.88, 132.20, 130.33, 129.59, 127.42, 126.21, 124.06, 123.75, 123.33, 123.05, 121.91, 119.88, 35.22, 31.34. $C_{25}H_{24}N_6O_2$. MS (ESI−): m/z 439.8 ([M − H]$^-$, 100). Combustion analysis measured (calculated): C 67.82 (68.17); H 5.57 (5.49); N 18.91 (19.08).

2-(4-(tert-Butyl)benzamido)-N-(3-carbamoylphenyl)benzamide (**28**). **13** (417 mg, 1.0 mmol, 1.0 equiv) was added to a mixture of silica gel and NH_4Cl (5:1, 1.3 g). After TsCl (210 mg, 1.1 mmol, 1.1 equiv) was added, the mixture was treated with 2.2 mL of triethylamine mixed with a spatula for 5 min. Then the mixture was added to 30 mL of ethyl acetate, and silica was filtered off. The filtrate was washed with 1% aqueous hydrochloric acid, and the aqueous layer was extracted with additional ethyl acetate three times. The combined aqueous layers were dried over Na_2SO_4, and the solvents were evaporated in vacuum. Further purification was performed by column chromatography on silica with hexane/ethyl acetate/acetic acid and recrystallization from acetone/water to obtain **28** as white solid in 38% yield. R_f (hexane/ethyl acetate/acetic acid (49:49:2)) = 0.34. ^{1}H NMR (500 MHz, DMSO) δ = 11.70 (s, 1H), 10.67 (s, 1H), 8.58−8.48 (m, 1H), 8.19 (t, J = 1.7 Hz, 1H), 8.01−7.95 (m, 2H), 7.88−7.83 (m, 3H), 7.67−7.62 (m, 2H), 7.62 7.58 (m, 2H), 7.46 (t, J = 7.9 Hz, 1H), 7.40 (s, 1H), 7.30 (td, J = 7.8, 1.0 Hz, 1H), 1.31 (s, 9H). ^{13}C NMR (126 MHz, DMSO) δ = 168.19, 168.09, 165.01, 155.51, 139.42, 138.94, 135.44, 132.90, 132.21, 129.53, 128.99, 127.35, 126.26, 124.49, 123.59, 123.53, 122.69, 121.57, 121.39, 35.22, 31.34. $C_{25}H_{25}N_3O_3$. MS (ESI−): m/z 414.26 ([M − H]$^-$, 100). Combustion analysis measured (calculated): C 71.93 (72.27); H 6.06 (6.07); N 9.76 (10.11).

2-(4-(tert-Butyl)benzamido)-N-(3,4-dimethoxyphenyl)benzamide (**29**). Preparation according to general procedure d using **7f** and *tert*-butylbenzoyl chloride (**8a**). After column chromatography on silica with hexane/ethyl acetate/acetic acid (89:9:2) as mobile phase, the product was recrystallized from hexane/ethyl acetate to give **29** as white solid in 70% yield. R_f (hexane/ethyl acetate/acetic acid (49:49:2)) = 0.57. ^{1}H NMR (500 MHz, DMSO) δ = 11.83 (s, 1H), 10.41 (s, 1H), 8.55 (d, J = 8.3 Hz, 1H), 7.93 (d, J = 7.7 Hz, 1H), 7.86 (d, J = 8.3 Hz, 2H), 7.63−7.58 (m, 3H), 7.35−7.25 (m, 3H), 6.96 (d, J = 8.6 Hz, 1H), 3.76 (s, 6H), 1.32 (s, 9H). ^{13}C NMR (126 MHz, DMSO) δ = 167.65, 164.92, 155.49, 148.94, 146.24, 139.38, 132.68, 132.22, 132.14, 129.28, 127.34, 126.24, 123.50, 122.72, 121.40, 114.03, 112.27, 106.96, 56.19, 55.95, 35.22, 31.34. $C_{26}H_{28}N_2O_4$. MS (ESI+): m/z 455.53 ([M + Na]$^+$, 100). Combustion analysis measured (calculated): C 71.87 (72.20); H 6.46 (6.53); N 6.46 (6.48).

2-(4-(tert-Butyl)benzamido)-N-(3,4,5-trimethoxyphenyl)-benzamide (**30**). Preparation according to general procedure d using **7g** and *tert*-butylbenzoyl chloride (**8a**). After column chromatography on silica with hexane/ethyl acetate/acetic acid (89:9:2) as mobile phase, the product was recrystallized from hexane/ethyl acetate to give **30** as white solid in 74% yield. R_f (hexane/ethyl acetate/acetic acid

dx.doi.org/10.1021/jm500937v | J. Med. Chem. XXXX, XXX, XXX−XXX

(49:49:2)) = 0.54. ^{1}H NMR (500 MHz, DMSO) δ = 11.59 (s, 1H), 10.43 (s, 1H), 8.47 (d, J = 8.3 Hz, 1H), 7.88 (dd, J = 12.9, 8.2 Hz, 3H), 7.64−7.56 (m, 3H), 7.29 (t, J = 7.4 Hz, 1H), 7.09 (s, 2H), 3.77 (s, 6H), 3.65 (s, 3H), 1.32 (s, 9H). ^{13}C NMR (126 MHz, DMSO) δ = 167.74, 165.02, 155.49, 153.10, 139.06, 134.91, 134.79, 132.66, 132.17, 129.36, 127.43, 126.20, 123.67, 123.48, 121.80, 99.73, 60.60, 56.32, 35.22, 31.35. $C_{27}H_{30}N_2O_5$. MS (ESI+): m/z 463.52 ([M + H]$^+$, 51); 485.51 ([M + Na]$^+$, 51). Combustion analysis measured (calculated): C 69.85 (70.11); H 6.47 (6.54); N 6.21 (6.06).

*2-(3-(2-(4-(tert-Butyl)benzamido)benzamido)phenyl)acetic Acid (**31**).* Preparation according to general procedure d using **7h** and *tert*-butylbenzoyl chloride (**8a**). After column chromatography on silica with hexane/ethyl acetate/acetic acid (89:9:2) as mobile phase, the product was recrystallized from hexane/ethyl acetate to give **31** as white solid in 72% yield. R_f (hexane/ethyl acetate/acetic acid (49:49:2)) = 0.48. ^{1}H NMR (500 MHz, DMSO) δ = 12.37 (s, 1H), 11.68 (s, 1H), 10.55 (s, 1H), 8.52 (d, J = 8.3 Hz, 1H), 7.94 (d, J = 7.8 Hz, 1H), 7.85 (d, J = 8.4 Hz, 2H), 7.66−7.62 (m, 2H), 7.60 (d, J = 8.2 Hz, 3H), 7.33 (t, J = 7.8 Hz, 1H), 7.29 (t, J = 7.6 Hz, 1H), 7.06 (d, J = 7.6 Hz, 1H), 3.58 (s, 2H), 1.32 (s, 9H). ^{13}C NMR (126 MHz, DMSO) δ = 173.06, 167.96, 165.00, 155.48, 139.33, 138.87, 135.98, 132.77, 132.22, 129.52, 127.37, 126.24, 125.92, 123.57, 122.92, 122.54, 121.54, 120.13, 67.49, 41.28, 35.22, 31.35. $C_{26}H_{26}N_2O_4$. MS (ESI−): m/z 429.17 ([M − H]$^-$, 100). Combustion analysis measured (calculated): C 72.35 (72.54); H 6.27 (6.09); N 6.19 (6.51).

*3-(3-(2-(4-(tert-Butyl)benzamido)benzamido)phenyl)propanoic Acid (**32**).* Preparation according to general procedure d using **7i** and *tert*-butylbenzoyl chloride (**8a**). After column chromatography on silica with hexane/ethyl acetate/acetic acid (89:9:2) as mobile phase, the product was recrystallized from hexane/ethyl acetate to give **32** as white solid in 72% yield. R_f (hexane/ethyl acetate/acetic acid (49:49:2)) = 0.55. ^{1}H NMR (500 MHz, DMSO) δ = 12.16 (s, 1H), 11.69 (s, 1H), 10.50 (s, 1H), 8.51 (d, J = 8.3 Hz, 1H), 7.96−7.91 (m, 1H), 7.85 (d, J = 8.4 Hz, 2H), 7.64−7.57 (m, 3H), 7.52 (s, 1H), 7.29 (ddd, J = 8.3, 3.1, 1.7 Hz, 2H), 7.03 (d, J = 7.6 Hz, 1H), 2.83 (t, J = 7.6 Hz, 2H), 2.55 (t, J = 7.6 Hz, 2H), 1.31 (s, 9H). ^{13}C NMR (126 MHz, DMSO) δ = 174.14, 167.92, 164.99, 155.49, 141.85, 139.31, 138.87, 132.75, 132.20, 129.47, 129.08, 127.36, 126.24, 124.74, 123.58, 122.97, 121.55, 121.54, 119.56, 35.55, 35.22, 31.34, 30.83. $C_{27}H_{28}N_2O_4$. MS (ESI+): m/z 467.52 ([M + Na]$^+$, 100). Combustion analysis measured (calculated): C 73.32 (72.95); H 6.50 (6.35); N 5.88 (6.30).

*3-(2-(4-(tert-Butyl)benzamido)benzamido)-4-methylbenzoic Acid (**33**).* Preparation according to general procedure d using **7j** and *tert*-butylbenzoyl chloride (**8a**). After column chromatography on silica with hexane/ethyl acetate/acetic acid (89:9:2) as mobile phase, the product was recrystallized from hexane/ethyl acetate to give **33** as white solid in 64% yield. R_f (hexane/ethyl acetate/acetic acid (49:49:2)) = 0.58. ^{1}H NMR (500 MHz, DMSO) δ = 12.96 (s, 1H), 12.03 (s, 1H), 10.38 (s, 1H), 8.61 (d, J = 8.3 Hz, 1H), 8.07 (d, J = 7.7 Hz, 1H), 7.91 (d, J = 1.2 Hz, 1H), 7.83 (d, J = 8.5 Hz, 2H), 7.79 (dd, J = 7.9, 1.5 Hz, 1H), 7.65 (t, J = 7.8 Hz, 1H), 7.58 (d, J = 8.5 Hz, 2H), 7.44 (d, J = 8.0 Hz, 1H), 7.30 (t, J = 7.6 Hz, 1H), 2.32 (s, 3H), 1.29 (s, 9H). ^{13}C NMR (126 MHz, DMSO) δ = 168.35, 167.38, 164.96, 155.48, 140.12, 139.94, 136.47, 133.11, 132.19, 131.23, 129.47, 129.41, 128.35, 127.77, 127.30, 126.25, 123.53, 121.44, 121.26, 40.57, 40.48, 40.41, 40.32, 40.24, 40.15, 40.07, 39.98, 39.91, 39.81, 39.65, 39.48, 35.20, 31.32, 31.17, 18.56. $C_{26}H_{26}N_2O_4$. MS (ESI−): m/z 429.9 ([M − H]$^-$, 100). Combustion analysis measured (calculated): C 72.21 (72.54); H 6.12 (6.09); N 6.41 (6.51).

*3-(2-(4-(tert-Butyl)benzamido)benzamido)-2-methylbenzoic Acid (**34**).* Preparation according to general procedure d using **7k** and *tert*-butylbenzoyl chloride (**8a**). After column chromatography on silica with hexane/ethyl acetate/acetic acid (89:9:2) as mobile phase, the product was recrystallized from hexane/ethyl acetate to give **34** as white solid in 71% yield. R_f (hexane/ethyl acetate/acetic acid (49:49:2)) = 0.57. ^{1}H NMR (500 MHz, DMSO) δ = 12.17 (s, 1H), 10.43 (s, 1H), 8.66 (d, J = 8.3 Hz, 1H), 8.09 (d, J = 7.7 Hz, 1H), 7.83 (d, J = 8.5 Hz, 2H), 7.74−7.69 (m, 1H), 7.68−7.62 (m, 1H), 7.58 (d, J = 8.5 Hz, 2H), 7.49 (d, J = 7.2 Hz, 1H), 7.35 (t, J = 7.8 Hz, 1H), 7.32−7.27 (m, 1H), 2.39 (s, 3H), 1.29 (s, 9H). ^{13}C NMR (126 MHz, DMSO) δ = 169.48, 168.48, 164.92, 155.51, 140.16, 137.30, 135.52, 133.27, 133.21, 132.17, 132.12, 131.11, 129.34, 128.58, 127.25, 126.29, 123.45, 121.08, 120.86, 35.20, 31.31, 15.74. $C_{26}H_{26}N_2O_4$. MS (ESI−): m/z 429.8 ([M − H]$^-$, 100). Combustion analysis measured (calculated): C 72.10 (72.54); H 6.06 (6.09); N 6.17 (6.51).

*5-(2-(4-(tert-Butyl)benzamido)benzamido)-2-methylbenzoic Acid (**35**).* Preparation according to general procedure d using **7l** and *tert*-butylbenzoyl chloride (**8a**). After column chromatography on silica with hexane/ethyl acetate/acetic acid (89:9:2) as mobile phase, the product was recrystallized from hexane/ethyl acetate to give **35** as white solid in 66% yield. R_f (hexane/ethyl acetate/acetic acid (49:49:2)) = 0.58. ^{1}H NMR (500 MHz, DMSO) δ = 12.91 (s, 1H), 11.65 (s, 1H), 10.61 (s, 1H), 8.50 (d, J = 8.3 Hz, 1H), 8.17 (d, J = 1.9 Hz, 1H), 7.94 (d, J = 7.8 Hz, 1H), 7.88−7.80 (m, 3H), 7.61 (dd, J = 17.6, 8.1 Hz, 3H), 7.29 (dd, J = 14.6, 7.8 Hz, 2H), 1.32 (s, 9H). ^{13}C NMR (126 MHz, DMSO) δ = 168.87, 167.96, 165.03, 155.48, 139.29, 136.73, 135.30, 132.80, 132.25, 130.94, 129.48, 127.37, 126.23, 124.89, 123.61, 123.44, 122.93, 121.63, 40.57, 40.48, 40.41, 40.32, 40.24, 40.15, 40.07, 39.98, 39.91, 39.81, 39.65, 39.48, 35.22, 31.35, 21.27. $C_{26}H_{26}N_2O_4$. MS (ESI+): m/z 431.46 ([M + H]$^+$, 16); 453.45 ([M + Na]$^+$, 100). Combustion analysis measured (calculated): C 72.19 (72.54); H 6.08 (6.09); N 6.43 (6.51).

*3-(2-(4-(tert-Butyl)benzamido)benzamido)-4-methoxybenzoic Acid (**36**).* Preparation according to general procedure d using **7m** and *tert*-butylbenzoyl chloride (**8a**). After column chromatography on silica with hexane/ethyl acetate/acetic acid (89:9:2) as mobile phase, the product was recrystallized from hexane/ethyl acetate to give **36** as white solid in 38% yield. R_f (hexane/ethyl acetate/acetic acid (49:49:2)) = 0.54. ^{1}H NMR (500 MHz, DMSO) δ = 11.83 (s, 1H), 9.93 (s, 1H), 8.49 (d, J = 8.3 Hz, 1H), 8.22 (t, J = 5.4 Hz, 1H), 8.01 (d, J = 7.7 Hz, 1H), 7.87−7.83 (m, 3H), 7.64 (t, J = 7.5 Hz, 1H), 7.58 (d, J = 8.4 Hz, 2H), 7.29 (t, J = 7.6 Hz, 1H), 7.20 (d, J = 8.7 Hz, 1H), 3.83 (s, 3H), 1.30 (s, 9H). ^{13}C NMR (126 MHz, DMSO) δ = 167.87, 167.29, 165.16, 156.35, 155.52, 139.36, 133.01, 132.11, 129.44, 128.98, 127.37, 127.09, 126.36, 126.22, 123.87, 123.20, 122.48, 121.89, 111.81, 56.52, 35.21, 31.33. $C_{26}H_{26}N_2O_5$. MS (ESI−): m/z 445.24 ([M − H]$^-$, 100). Combustion analysis measured (calculated): C 69.54 (69.94); H 5.92 (5.87); N 6.01 (6.27).

*3-(2-(4-(tert-Butyl)benzamido)benzamido)-4-fluorobenzoic Acid (**37**).* Preparation according to general procedure d using **7n** and *tert*-butylbenzoyl chloride (**8a**). After column chromatography on silica with hexane/ethyl acetate/acetic acid (89:9:2) as mobile phase, the product was recrystallized from hexane/ethyl acetate to give **37** as white solid in 51% yield. R_f (hexane/ethyl acetate/acetic acid (49:49:2)) = 0.59. ^{1}H NMR (500 MHz, DMSO) δ = 13.18 (s, 1H), 11.81 (s, 1H), 10.58 (s, 1H), 8.56 (d, J = 8.2 Hz, 1H), 8.15 (dd, J = 7.3, 2.0 Hz, 1H), 8.01 (t, J = 10.3 Hz, 1H), 7.90 (ddd, J = 8.4, 4.6, 2.1 Hz, 1H), 7.83 (d, J = 8.5 Hz, 2H), 7.68−7.63 (m, 1H), 7.58 (d, J = 8.4 Hz, 2H), 7.49−7.43 (m, 1H), 7.30 (dd, J = 11.2, 4.0 Hz, 1H), 1.30 (s, 9H). ^{13}C NMR (126 MHz, DMSO) δ = 168.29, 166.60, 165.08, 155.51, 139.78, 133.34, 132.17, 129.65, 129.38, 129.31, 129.13, 127.77, 127.33, 126.24, 125.87, 125.77, 123.62, 121.48, 121.33, 116.99, 116.82, 35.20, 31.32. $C_{25}H_{23}FN_2O_4$. MS (ESI+): m/z 435.44 ([M + H]$^+$, 13); 457.45 ([M + Na]$^+$, 100). Combustion analysis measured (calculated): C 68.92 (69.11); H 5.24 (5.34); N 6.49 (6.45).

*3-(2-(4-(tert-Butyl)benzamido)benzamido)-4-chlorobenzoic Acid (**38**).* Preparation according to general procedure d using **7o** and *tert*-butylbenzoyl chloride (**8a**). After column chromatography on silica with hexane/ethyl acetate/acetic acid (89:9:2) as mobile phase, the product was recrystallized from hexane/ethyl acetate to give **38** as white solid in 35% yield. R_f (hexane/ethyl acetate/acetic acid (49:49:2)) = 0.61. ^{1}H NMR (500 MHz, DMSO) δ = 13.33 (s, 1H), 11.87 (s, 1H), 10.56 (s, 1H), 8.57 (d, J = 8.3 Hz, 1H), 8.12 (d, J = 1.8 Hz, 1H), 8.06 (d, J = 7.6 Hz, 1H), 7.88 (dd, J = 8.4, 1.8 Hz, 1H), 7.84 (d, J = 8.3 Hz, 2H), 7.73 (d, J = 8.4 Hz, 1H), 7.66 (t, J = 7.6 Hz, 1H), 7.58 (d, J = 8.3 Hz, 2H), 7.31 (t, J = 7.6 Hz, 1H), 1.30 (s, 9H). ^{13}C NMR (126 MHz, DMSO) δ = 168.37, 166.65, 165.06, 155.51, 139.85, 135.32, 135.26, 133.35, 132.15, 130.86, 130.56, 129.94, 129.46, 129.04, 127.35, 126.24, 123.66, 121.49, 121.33, 35.21, 31.32. $C_{25}H_{23}ClN_2O_4$.

dx.doi.org/10.1021/jm500937v | J. Med. Chem. XXXX, XXX, XXX−XXX

MS (ESI+): m/z 474.44 ([M + H]$^+$, 100). Combustion analysis measured (calculated): C 66.38 (66.59); H 5.17 (5.14); N 6.14 (6.21).

*5-(2-(4-(tert-Butyl)benzamido)benzamido)-2-methoxybenzoic Acid (**39**).* Preparation according to general procedure d using **7p** and *tert*-butylbenzoyl chloride (**8a**). After column chromatography on silica with hexane/ethyl acetate/acetic acid (89:9:2) as mobile phase, the product was recrystallized from hexane/ethyl acetate to give **39** as white solid in 60% yield. R_f (hexane/ethyl acetate/acetic acid (49:49:2)) = 0.40. ^{1}H NMR (500 MHz, DMSO) δ = 11.76 (s, 1H), 10.53 (s, 1H), 8.53 (d, J = 7.7 Hz, 1H), 7.97 (d, J = 2.6 Hz, 1H), 7.94 (dd, J = 7.9, 1.2 Hz, 1H), 7.87−7.82 (m, 3H), 7.64−7.58 (m, 3H), 7.28 (td, J = 7.8, 1.1 Hz, 1H), 7.15 (d, J = 9.1 Hz, 1H), 3.82 (s, 3H), 1.32 (s, 9H). ^{13}C NMR (126 MHz, DMSO) δ = 167.78, 167.50, 164.99, 155.49, 155.36, 139.40, 132.78, 132.25, 131.34, 129.37, 127.34, 126.56, 126.25, 124.37, 123.55, 122.60, 121.47, 113.25, 56.48, 35.23, 31.35. $C_{26}H_{26}N_2O_5$. MS (ESI−): m/z 445.9 ([M − H]$^-$, 100). Combustion analysis measured (calculated): C 69.77 (69.94); H 5.93 (5.87); N 5.93 (6.27).

*5-(2-(4-(tert-Butyl)benzamido)benzamido)-2-chlorobenzoic Acid (**40**).* Preparation according to general procedure d using **7q** and *tert*-butylbenzoyl chloride (**8a**). After column chromatography on silica with hexane/ethyl acetate/acetic acid (89:9:2) as mobile phase, the product was recrystallized from hexane/ethyl acetate to give **40** as white solid in 63% yield. R_f (hexane/ethyl acetate/acetic acid (49:49:2)) = 0.50. ^{1}H NMR (500 MHz, DMSO) δ = 11.42 (s, 1H), 10.74 (s, 1H), 8.41 (d, J = 7.9 Hz, 1H), 8.17 (d, J = 2.6 Hz, 1H), 7.91 (dd, J = 8.7, 2.3 Hz, 2H), 7.85 (d, J = 8.5 Hz, 2H), 7.65−7.61 (m, 1H), 7.59 (d, J = 8.5 Hz, 2H), 7.55 (d, J = 8.7 Hz, 1H), 7.33−7.27 (m, 1H), 1.32 (s, 9H). ^{13}C NMR (126 MHz, DMSO) δ = 172.49, 168.03, 166.91, 165.13, 155.46, 139.02, 138.08, 132.85, 131.77, 131.44, 129.52, 127.44, 126.79, 126.17, 125.07, 123.77, 123.52, 123.37, 122.03, 35.22, 31.35. $C_{25}H_{23}ClN_2O_4$. MS (ESI−): m/z 449.9 ([M − H]$^-$, 100). Combustion analysis measured (calculated): C 66.53 (66.59); H 5.19 (5.14); N 6.23 (6.21).

*2-Bromo-5-(2-(4-(tert-butyl)benzamido)benzamido)benzoic Acid (**41**).* Preparation according to general procedure d using **7r** and *tert*-butylbenzoyl chloride (**8a**). After column chromatography on silica with hexane/ethyl acetate/acetic acid (89:9:2) as mobile phase, the product was recrystallized from hexane/ethyl acetate to give **41** as white solid in 54% yield. R_f (hexane/ethyl acetate/acetic acid (49:49:2)) = 0.48. ^{1}H NMR (500 MHz, DMSO) δ = 11.40 (s, 1H), 10.73 (s, 1H), 8.41 (t, J = 7.3 Hz, 1H), 8.13 (d, J = 2.6 Hz, 1H), 7.91 (d, J = 7.7 Hz, 1H), 7.83 (dd, J = 13.6, 5.5 Hz, 3H), 7.71 (d, J = 8.7 Hz, 1H), 7.63 (t, J = 7.8 Hz, 1H), 7.59 (d, J = 8.4 Hz, 2H), 7.30 (t, J = 7.4 Hz, 1H), 1.32 (s, 9H). ^{13}C NMR (126 MHz, DMSO) δ = 168.03, 167.52, 165.14, 155.47, 139.00, 138.62, 134.58, 134.09, 132.85, 132.21, 129.52, 127.44, 126.17, 125.03, 123.79, 123.58, 123.21, 122.06, 114.61, 35.22, 31.35. $C_{25}H_{23}BrN_2O_4$. MS (ESI−): m/z 494.0 ([M − H]$^-$, 99), 495.9 ([M − H]$^-$, 100). Combustion analysis measured (calculated): C 60.93 (60.62); H 5.11 (4.68); N 5.60 (5.66).

*5-(2-(4-(tert-Butyl)benzamido)benzamido)-2-nitrobenzoic Acid (**42**).* Preparation according to general procedure d using **7s** and *tert*-butylbenzoyl chloride (**8a**). After column chromatography on silica with hexane/ethyl acetate/acetic acid (89:9:2) as mobile phase, the product was recrystallized from hexane/ethyl acetate to give **42** as yellow solid in 31% yield. R_f (hexane/ethyl acetate/acetic acid (49:49:2)) = 0.51. ^{1}H NMR (500 MHz, DMSO) δ = 12.23 (s, 1H), 10.58 (s, 1H), 8.44 (d, J = 2.6 Hz, 1H), 8.25 (t, J = 1.8 Hz, 1H), 7.97 (t, J = 8.5 Hz, 1H), 7.94−7.91 (m, 1H), 7.86 (d, J = 8.5 Hz, 2H), 7.75−7.71 (m, 1H), 7.61 (d, J = 8.5 Hz, 2H), 7.55 (t, J = 7.9 Hz, 1H), 6.98 (dd, J = 8.9, 2.6 Hz, 1H), 1.32 (s, 9H). ^{13}C NMR (126 MHz, DMSO) δ = 174.03, 168.09, 167.60, 165.19, 162.65, 153.22, 142.08, 138.89, 134.14, 131.45, 129.87, 127.64, 126.67, 124.82, 125.61, 122.34, 113.12, 109.34, 106.03, 35.23, 31.33. $C_{25}H_{23}N_3O_6$. MS (ESI−): m/z 460.9 ([M − H]$^-$, 100). Combustion analysis measured (calculated): C 64.78 (65.07); H 4.97 (5.02); N 9.06 (9.11).

*3-(2-(4-(tert-Butyl)benzamido)-6-chlorobenzamido)benzoic Acid (**43**).* Preparation according to general procedure d using **7t** and *tert*-butylbenzoyl chloride (**8a**). After column chromatography on silica with hexane/ethyl acetate/acetic acid (89:9:2) as mobile phase, the product was recrystallized from hexane/ethyl acetate to give **43** as white solid in 68% yield. R_f (hexane/ethyl acetate/acetic acid (49:49:2)) = 0.47. ^{1}H NMR (500 MHz, DMSO) δ = 12.96 (s, 1H), 10.50 (s, 1H), 10.11 (s, 1H), 8.32 (s, 1H), 7.87 (t, J = 7.7 Hz, 3H), 7.75 (d, J = 8.0 Hz, 1H), 7.64 (t, J = 7.2 Hz, 2H), 7.49 (dd, J = 15.4, 8.0 Hz, 3H), 7.42 (t, J = 7.9 Hz, 1H), 1.30 (s, 9H). ^{13}C NMR (126 MHz, DMSO) δ = 167.60, 166.01, 165.55, 155.13, 139.86, 137.43, 133.59, 132.99, 131.72, 131.69, 131.52, 129.36, 128.42, 128.05, 127.73, 125.67, 124.86, 124.32, 121.01, 35.15, 31.37. $C_{25}H_{23}ClN_2O_4$. MS (ESI−): m/z 449.08 ([M − H]$^-$, 100). Combustion analysis measured (calculated): C 66.42 (66.59); H 5.10 (5.14); N 6.17 (6.21).

*3-(2-(4-(tert-Butyl)benzamido)-3-chlorobenzamido)benzoic Acid (**44**).* Preparation according to general procedure e using **44a**. After column chromatography on silica with hexane/ethyl acetate/acetic acid (89:9:2) as mobile phase, the product was recrystallized from hexane/ethyl acetate to give **44** as white solid in 86% yield. R_f (hexane/ethyl acetate/acetic acid (49:49:2)) = 0.46. ^{1}H NMR (500 MHz, DMSO) δ = 12.95 (s, 1H), 10.50 (s, 1H), 10.11 (s, 1H), 8.32 (s, 1H), 7.90−7.84 (m, 3H), 7.75 (dd, J = 8.1, 1.2 Hz, 1H), 7.67−7.61 (m, 2H), 7.52−7.46 (m, 3H), 7.42 (t, J = 7.9 Hz, 1H), 1.30 (s, 9H). ^{13}C NMR (126 MHz, DMSO) δ = 167.59, 166.01, 165.55, 155.13, 139.85, 137.43, 133.58, 132.98, 131.72, 131.69, 131.52, 129.36, 128.41, 128.05, 127.72, 125.67, 124.85, 124.32, 121.01, 35.15, 31.37. $C_{25}H_{23}ClN_2O_4$. MS (ESI−): m/z 449.7 ([M − H]$^-$, 100). Combustion analysis measured (calculated): C 66.48 (66.59); H 5.11 (5.14); N 6.12 (6.21).

*3-(2-(4-(tert-Butyl)benzamido)-5-chlorobenzamido)benzoic Acid (**45**).* Preparation according to general procedure d using **7u** and *tert*-butylbenzoyl chloride (**8a**). After column chromatography on silica with hexane/ethyl acetate/acetic acid (89:9:2) as mobile phase, the product was recrystallized from hexane/ethyl acetate to give **45** as pale-yellow solid in 44% yield. R_f (hexane/ethyl acetate/acetic acid (49:49:2)) = 0.65. ^{1}H NMR (500 MHz, DMSO) δ = 11.45 (s, 1H), 10.76 (s, 1H), 8.45 (d, J = 8.9 Hz, 1H), 8.30 (s, 1H), 8.01 (d, J = 2.4 Hz, 1H), 7.99−7.96 (m, 1H), 7.84 (d, J = 8.5 Hz, 2H), 7.73 (d, J = 7.8 Hz, 1H), 7.70 (dd, J = 8.9, 2.5 Hz, 1H), 7.59 (d, J = 8.5 Hz, 2H), 7.51 (t, J = 7.9 Hz, 1H), 1.31 (s, 9H). ^{13}C NMR (126 MHz, DMSO) δ = 167.55, 166.61, 165.16, 155.63, 139.08, 137.98, 132.39, 131.96, 131.77, 129.45, 129.15, 127.52, 127.47, 126.22, 125.64, 125.60, 125.12, 123.66, 122.33, 35.24, 31.33. $C_{25}H_{23}ClN_2O_4$. MS (ESI−): m/z 449.8 ([M − H]$^-$, 100). Combustion analysis measured (calculated): C 66.25 (66.59); H 4.96 (5.14); N 6.12 (6.21).

*3-(2-(4-(tert-Butyl)benzamido)-4-chlorobenzamido)benzoic Acid (**46**).* Preparation according to general procedure d using **7v** and *tert*-butylbenzoyl chloride (**8a**). After column chromatography on silica with hexane/ethyl acetate/acetic acid (89:9:2) as mobile phase, the product was recrystallized from hexane/ethyl acetate to give **46** as white solid in 61% yield. R_f (hexane/ethyl acetate/acetic acid (49:49:2)) = 0.63. ^{1}H NMR (500 MHz, DMSO) δ = 13.05 (s, 1H), 11.82−11.68 (m, 1H), 10.76 (s, 1H), 8.63 (d, J = 2.1 Hz, 1H), 8.32 (d, J = 16.3 Hz, 1H), 8.03−7.96 (m, 2H), 7.85 (d, J = 8.4 Hz, 2H), 7.74 (d, J = 7.8 Hz, 1H), 7.61 (d, J = 8.5 Hz, 2H), 7.52 (t, J = 7.9 Hz, 1H), 7.43−7.36 (m, 1H), 1.31 (s, 9H). ^{13}C NMR (126 MHz, DMSO) δ = 167.54, 167.28, 165.31, 155.82, 140.69, 139.04, 137.28, 131.81, 131.75, 131.33, 129.47, 127.46, 126.31, 125.82, 125.64, 123.32, 122.45, 121.28, 120.88, 35.26, 31.32. $C_{25}H_{23}ClN_2O_4$. MS (ESI−): m/z 449.8 ([M − H]$^-$, 100). Combustion analysis measured (calculated): C 66.68 (66.59); H 5.05 (5.14); N 6.08 (6.21).

*3-(2-(4-(tert-Butyl)benzamido)-5-methoxybenzamido)benzoic Acid (**47**).* Preparation according to general procedure e using **47a**. After column chromatography on silica with hexane/ethyl acetate/acetic acid (89:9:2) as mobile phase, the product was recrystallized from hexane/ethyl acetate to give **47** as white solid in 85% yield. R_f (hexane/ethyl acetate/acetic acid (49:49:2)) = 0.54. ^{1}H NMR (500 MHz, DMSO) δ = 13.04 (s, 1H), 11.13 (s, 1H), 10.64 (s, 1H), 8.31 (d, J = 1.7 Hz, 1H), 8.26 (d, J = 9.0 Hz, 1H), 8.00−7.94 (m, 1H), 7.83 (d, J = 8.5 Hz, 2H), 7.71 (d, J = 7.8 Hz, 1H), 7.57 (d, J = 8.5 Hz, 2H), 7.50 (t, J = 7.9 Hz, 1H), 7.45 (d, J = 2.9 Hz, 1H), 7.22 (dd, J = 9.0, 2.9 Hz, 1H), 3.87 (s, 3H), 1.31 (s, 9H). ^{13}C NMR (126 MHz, DMSO) δ = 167.57, 167.53, 164.88, 155.38, 155.21, 139.27, 132.32, 131.90,

dx.doi.org/10.1021/jm500937v | J. Med. Chem. XXXX, XXX, XXX−XXX

131.68, 129.42, 127.34, 126.09, 125.61, 125.58, 125.42, 124.06, 122.24, 118.05, 114.42, 56.07, 35.18, 31.36. $C_{26}H_{26}N_2O_5$. MS (ESI−): m/z 446.1 ([M − H]$^-$, 100). Combustion analysis measured (calculated): C 69.83 (69.94); H 6.02 (5.87); N 6.05 (6.27).

*3-(2-(4-(tert-Butyl)benzamido)-4-nitrobenzamido)benzoic Acid (**48**).* Preparation according to general procedure d using **7w** and *tert*-butylbenzoyl chloride (**8a**). After column chromatography on silica with hexane/ethyl acetate/acetic acid (89:9:2) as mobile phase, the product was recrystallized from hexane/ethyl acetate to give **48** as yellow solid in 51% yield. R_f (hexane/ethyl acetate/acetic acid (49:49:2)) = 0.56. ^{1}H NMR (500 MHz, DMSO) δ = 11.50 (s, 1H), 10.95 (s, 1H), 9.24 (d, J = 2.2 Hz, 1H), 8.33 (s, 1H), 8.16 (d, J = 8.6 Hz, 1H), 8.12 (dd, J = 8.6, 2.3 Hz, 1H), 7.99 (dd, J = 8.1, 1.0 Hz, 1H), 7.88−7.85 (m, 2H), 7.76−7.73 (m, 1H), 7.62−7.59 (m, 2H), 7.52 (t, J = 7.9 Hz, 1H), 1.31 (s, 9H). ^{13}C NMR (126 MHz, DMSO) δ = 172.49, 167.52, 166.29, 165.57, 162.77, 155.92, 149.51, 139.71, 139.02, 131.77, 131.56, 131.08, 129.51, 129.25, 127.62, 126.25, 125.75, 125.63, 122.29, 118.13, 116.32, 35.26, 31.31. $C_{25}H_{23}N_3O_6$. MS (ESI−): m/z 460.9 ([M − H]$^-$, 100). Combustion analysis measured (calculated): C 64.80 (65.07); H 5.17 (5.02); N 9.06 (9.11).

*3-(2-(4-(tert-Butyl)benzamido)-4-methylbenzamido)benzoic Acid (**49**).* Preparation according to general procedure e using **49a**. After column chromatography on silica with hexane/ethyl acetate/acetic acid (89:9:2) as mobile phase, the product was recrystallized from hexane/ethyl acetate to give **49** as white solid in 82% yield. R_f (hexane/ethyl acetate/acetic acid (49:49:2)) = 0.60. ^{1}H NMR (500 MHz, DMSO) δ = 13.04 (s, 1H), 11.77 (s, 1H), 10.63 (s, 1H), 8.41 (s, 1H), 8.30 (s, 1H), 7.97 (dd, J = 9.0, 8.0 Hz, 1H), 7.88 (t, J = 7.3 Hz, 1H), 7.85 (d, J = 8.5 Hz, 2H), 7.72 (d, J = 7.8 Hz, 1H), 7.60 (d, J = 8.5 Hz, 2H), 7.51 (t, J = 7.9 Hz, 1H), 7.11 (d, J = 8.0 Hz, 1H), 2.42 (s, 3H), 1.32 (s, 9H). ^{13}C NMR (126 MHz, DMSO) δ = 168.20, 167.59, 164.97, 155.48, 143.26, 139.65, 139.20, 132.29, 129.52, 129.41, 127.31, 126.26, 125.79, 125.45, 124.18, 122.45, 121.81, 119.56, 35.23, 31.34, 21.94. $C_{26}H_{26}N_2O_4$. MS (ESI+): m/z 431.50 ([M + H]$^+$, 45), 453.49 ([M + Na]$^+$, 100). Combustion analysis measured (calculated): C 72.19 (72.54); H 6.33 (6.09); N 6.12 (6.51).

*3-(4-Bromo-2-(4-(tert-butyl)benzamido)benzamido)benzoic Acid (**50**).* Preparation according to general procedure d using **7x** and *tert*-butylbenzoyl chloride (**8a**). After column chromatography on silica with hexane/ethyl acetate/acetic acid (89:9:2) as mobile phase, the product was recrystallized from hexane/ethyl acetate to give **50** as white solid in 57% yield. R_f (hexane/ethyl acetate/acetic acid (49:49:2)) = 0.61. ^{1}H NMR (500 MHz, DMSO) δ = 11.70 (s, 1H), 10.76 (s, 1H), 8.76 (d, J = 2.0 Hz, 1H), 8.30 (t, J = 1.8 Hz, 1H), 7.97 (dt, J = 13.7, 6.8 Hz, 1H), 7.92 (d, J = 8.5 Hz, 1H), 7.85 (d, J = 8.5 Hz, 2H), 7.76−7.71 (m, 1H), 7.61 (d, J = 8.5 Hz, 2H), 7.52 (dd, J = 8.9, 7.1 Hz, 2H), 1.31 (s, 9H). ^{13}C NMR (126 MHz, DMSO) δ = 172.49, 167.54, 167.36, 165.29, 155.81, 140.62, 139.04, 131.80, 131.73, 131.39, 129.48, 127.46, 126.30, 126.09, 125.80, 125.63, 123.86, 122.43, 121.75, 35.26, 31.32. $C_{25}H_{23}BrN_2O_4$. MS (ESI+): m/z 517.47 ([M + Na]$^+$, 77), 519.46 ([M + Na]$^+$, 100). Combustion analysis measured (calculated): C 60.89 (60.62); H 4.72 (4.68); N 5.27 (5.66).

*3-(2-(4-(tert-Butyl)benzamido)-4-methoxybenzamido)benzoic Acid (**51**).* Preparation according to general procedure e using **51a**. After column chromatography on silica with hexane/ethyl acetate/acetic acid (89:9:2) as mobile phase, the product was recrystallized from hexane/ethyl acetate to give **51** as white solid in 83% yield. R_f (hexane/ethyl acetate/acetic acid (49:49:2)) = 0.56. ^{1}H NMR (500 MHz, DMSO) δ = 12.26 (s, 1H), 10.56 (s, 1H), 8.34 (d, J = 2.6 Hz, 1H), 8.26 (t, J = 1.8 Hz, 1H), 8.01 (t, J = 8.5 Hz, 1H), 7.99−7.95 (m, 1H), 7.86 (d, J = 8.5 Hz, 2H), 7.74−7.70 (m, 1H), 7.61 (d, J = 8.5 Hz, 2H), 7.50 (t, J = 7.9 Hz, 1H), 6.86 (dd, J = 8.9, 2.6 Hz, 1H), 3.88 (s, 3H), 1.32 (s, 9H). ^{13}C NMR (126 MHz, DMSO) δ = 168.18, 167.65, 165.13, 162.94, 155.62, 142.11, 139.13, 132.21, 131.32, 129.33, 127.29, 126.34, 125.82, 125.42, 122.63, 113.50, 108.95, 105.96, 55.99, 35.25, 31.33. $C_{26}H_{26}N_2O_5$. MS (ESI−): m/z 446.0 ([M − H]$^-$, 100). Combustion analysis measured (calculated): C 70.26 (69.94); H 5.88 (5.87); N 6.36 (6.27).

*5-(2-(4-(tert-Butyl)benzamido)-4-chlorobenzamido)-2-methylbenzoic Acid (**52**).* Preparation according to general procedure d using **7y** and *tert*-butylbenzoyl chloride (**8a**). After column chromatography on silica with hexane/ethyl acetate/acetic acid (89:9:2) as mobile phase, the product was recrystallized from hexane/ethyl acetate to give **52** as white solid in 74% yield. R_f (hexane/ethyl acetate/acetic acid (49:49:2)) = 0.63. ^{1}H NMR (500 MHz, DMSO) δ = 12.88 (s, 1H), 11.83 (d, J = 18.3 Hz, 1H), 10.67 (s, 1H), 8.65 (t, J = 2.6 Hz, 1H), 8.15 (t, J = 3.0 Hz, 1H), 8.00 (d, J = 8.5 Hz, 1H), 7.86−7.83 (m, 2H), 7.82 (dd, J = 8.3, 2.5 Hz, 1H), 7.61 (t, J = 6.4 Hz, 2H), 7.37 (dt, J = 13.0, 6.5 Hz, 1H), 7.30 (t, J = 11.2 Hz, 1H), 2.51 (s, 3H), 1.31 (s, 9H). ^{13}C NMR (126 MHz, DMSO) δ = 168.81, 167.16, 165.27, 155.82, 140.76, 137.25, 136.50, 135.53, 132.29, 131.80, 131.23, 130.94, 127.43, 126.31, 125.03, 123.58, 123.25, 121.00, 120.74, 35.26, 31.32, 21.28. $C_{26}H_{25}ClN_2O_4$. MS (ESI−): m/z 463.9 ([M − H]$^-$, 100). Combustion analysis measured (calculated): C 66.98 (67.17); H 5.73 (5.42); N 5.65 (6.03).

*5-(2-(4-(tert-Butyl)benzamido)-4-methoxybenzamido)-2-methylbenzoic Acid (**53**).* Preparation according to general procedure d using **7z** and *tert*-butylbenzoyl chloride (**8a**). After column chromatography on silica with hexane/ethyl acetate/acetic acid (89:9:2) as mobile phase, the product was recrystallized from hexane/ethyl acetate to give **53** as white solid in 63% yield. R_f (hexane/ethyl acetate/acetic acid (49:49:2)) = 0.59. ^{1}H NMR (500 MHz, DMSO) δ = 12.90 (s, 1H), 12.33 (s, 1H), 10.47 (s, 1H), 8.35 (d, J = 2.6 Hz, 1H), 8.13 (d, J = 2.4 Hz, 1H), 8.01 (d, J = 8.9 Hz, 1H), 7.88−7.84 (m, 2H), 7.83 (dd, J = 8.3, 2.4 Hz, 1H), 7.61 (d, J = 8.5 Hz, 2H), 7.31 (d, J = 8.4 Hz, 1H), 6.84 (dd, J = 8.9, 2.6 Hz, 1H), 3.88 (s, 3H), 2.51 (s, 3H), 1.31 (s, 9H). ^{13}C NMR (126 MHz, DMSO) δ = 168.87, 168.08, 165.11, 162.89, 155.60, 142.13, 136.69, 135.25, 132.23, 131.20, 130.91, 127.28, 126.33, 125.22, 123.73, 113.38, 108.91, 105.88, 55.97, 35.24, 31.33, 21.27. $C_{27}H_{28}N_2O_5$. MS (ESI−): m/z 459.2 ([M − H]$^-$, 100). Combustion analysis measured (calculated): C 70.12 (70.42); H 6.07 (6.13); N 5.89 (6.08).

*5-(2-(4-(tert-Butyl)benzamido)-4-methylbenzamido)-2-methylbenzoic Acid (**54**).* Preparation according to general procedure d using **7aa** and *tert*-butylbenzoyl chloride (**8a**). After column chromatography on silica with hexane/ethyl acetate/acetic acid (89:9:2) as mobile phase, the product was recrystallized from hexane/ethyl acetate to give **54** as white solid in 60% yield. R_f (hexane/ethyl acetate/acetic acid (49:49:2)) = 0.57. ^{1}H NMR (500 MHz, DMSO) δ = 11.86 (s, 1H), 10.54 (s, 1H), 8.43 (s, 1H), 8.15 (d, J = 2.3 Hz, 1H), 7.88 (d, J = 8.1 Hz, 1H), 7.85 (d, J = 8.5 Hz, 2H), 7.82 (dd, J = 8.5, 2.4 Hz, 1H), 7.60 (d, J = 8.5 Hz, 2H), 7.31 (d, J = 8.4 Hz, 1H), 7.10 (d, J = 8.0 Hz, 1H), 2.50 (s, 3H), 2.41 (s, 3H), 1.32 (s, 9H). ^{13}C NMR (126 MHz, DMSO) δ = 168.87, 168.08, 164.93, 155.48, 143.20, 139.70, 136.68, 135.27, 132.24, 131.56, 130.95, 129.42, 127.29, 126.27, 125.02, 124.12, 123.56, 121.68, 119.35, 35.22, 31.34, 21.94, 21.26. $C_{27}H_{28}N_2O_4$. MS (ESI−): m/z 444.0 ([M − H]$^-$, 100). Combustion analysis measured (calculated): C 72.95 (72.95); H 6.25 (6.35); N 5.91 (6.30).

Intermediates. *3-(2-Aminobenzamido)benzoic Acid (**7a**).* Preparation according to general procedure a1 using isatoic anhydride (**5a**) and 3-aminobenzoic acid (**4a**). The crude product was purified by column chromatography on silica with hexane/ethyl acetate/acetic acid (49:49:2) as mobile phase to obtain **7a** as white solid in 64% yield. R_f (hexane/ethyl acetate/acetic acid (49:49:2)) = 0.58. ^{1}H NMR (500 MHz, DMSO) δ = 13.16 (s, 1H), 7.96 (t, J = 8.0 Hz, 1H), 7.70 (dd, J = 9.1, 7.4 Hz, 1H), 7.65 (dd, J = 7.7, 1.2 Hz, 1H), 7.59 (t, J = 7.8 Hz, 1H), 7.53−7.49 (m, 1H), 7.37−7.31 (m, 1H), 7.05 (s, 1H), 6.79−6.70 (m, 2H). ^{13}C NMR (126 MHz, DMSO) δ = 167.26, 163.21, 147.09, 139.23, 135.33, 134.20, 132.11, 131.47, 129.79, 129.03, 128.32, 117.72, 115.09, 114.63. $C_{14}H_{12}N_2O_3$. MS (ESI−): m/z 255.0 ([M − H]$^-$, 100), as representative intermediate. For synthesis and analytical data of other intermediates, please see Supporting Information.

Docking. Docking simulations were performed using the Molecular Operating Environment (MOE) (version 2012.10; The Chemical Computing Group, Montreal, Canada). The crystal structure of FXR (PDB ID: 3OLF[32]) was downloaded from the Protein Data Bank (PDB). Prior to ligand docking, one monomer of the dimer crystal structure was isolated and the crystallized ligand was removed. Subsequently, the structure was prepared with Protonate 3D, and the active site was isolated using MOE Site Finder. The structures were

dx.doi.org/10.1021/jm500937v | J. Med. Chem. XXXX, XXX, XXX−XXX

placed in the site with the Triangle Matcher method and then ranked with the London dG scoring function. For the energy minimization in the pocket, MOE Force Field Refinement was used and ranked with the GBVI/WSA dG scoring function.

In Vitro Biological Evaluation. *FXR Transactivation Assay. Cell Culture.* HeLa cells were grown in DMEM high glucose, supplemented with 10% fetal calf serum (FCS), 1 mM sodium pyruvate (SP), penicillin (100 U/mL), and streptomycin (100 μg/mL) at 37 °C and 5% CO_2.

Plasmids for Full-Length FXR Transactivation Aassay. pcDNA3-hFXR contains the sequence of human FXR and was already published elsewhere,[43] and pGL3basic (Promega, Mannheim, Germany) was used as a reporter plasmid, with a shortened construct of the promotor of the bile salt export pump (BSEP, sequence of construct from ref 44) cloned into the SacI/NheI cleavage site in front of the luciferase gene. pRL-SV40 (Promega) was transfected as a control for normalization of transfection efficiency and cell growth. pSG5-hRXR was already published elsewhere[45] as well.

Full-Length FXR Transactivation Assay. Twenty-four h before transfection, HeLa cells were seeded in 96-well plates with a density of 8000 cells per well. Then 3.5 h before transfection, medium was changed to DMEM high glucose supplemented with 1 mM SP, penicillin (100 U/mL), streptomycin (100 μg/mL), and 0.5% charcoal-stripped FCS. Transient transfection of HeLa cells with BSEP-pGL3, pRL-SV40, and the expression plasmids pcDNA3-hFXR and pSG5-hRXR was carried out using calcium phosphate transfection method. Then 16 h after transfection, medium was changed to DMEM high glucose, supplemented with 1 mM SP, penicillin (100 U/mL), streptomycin (100 μg/mL), and 0.5% charcoal-stripped FCS. Then 24 h after transfection, medium was changed to DMEM without phenol red, supplemented with 1 mM SP, penicillin (100 U/mL), streptomycin (100 μg/mL), 2 mM L-glutamate, and 0.5% charcoal-stripped FCS, now additionally containing 0.1% DMSO and the respective test compound or 0.1% DMSO alone as untreated control. Each concentration was tested in triplicate wells, and each experiment was repeated independently at least three times. Following 24 h incubation with the test compounds, cells were assayed for luciferase activity using Dual-Glo luciferase assay system (Promega) according to the manufacturer's protocol. Luminescence was measured with a Tecan Infinite M200 luminometer (Tecan Deutschland GmbH, Crailsheim, Germany). Normalization of transfection efficacy and cell growth was done by division of firefly luciferase data by renilla luciferase data, resulting in relative light units (RLU). Fold activation was obtained by dividing the mean RLU of the tested compound at a respective concentration by the mean RLU of untreated control. Relative activation was obtained by dividing the fold activation of the tested compound at a respective concentration by the fold activation of FXR full agonist GW4064 (**3**) at 3 μM. EC_{50} and standard error of the mean values were calculated with the mean relative activation values of at least three independent experiments by SigmaPlot 10.0 (Systat Software GmbH, Erkrath, Germany) using a four parameter logistic regression.

FXR Target Gene Quantification (qRT-PCR). *Cell Culture.* HepG2 cells were seeded and grown in DMEM high glucose, supplemented with 10% FCS, 1 mM SP, penicillin (100 U/mL), and streptomycin (100 μg/mL) at 37 °C and 5% CO_2 in 6-well plates (2×10^6 per well). HT-29 cells were seeded and grown in McCoys 5A medium supplemented with 10% FCS, penicillin (100 U/mL), and streptomycin (100 μg/mL) at 37 °C and 5% CO_2 in 6-well plates (2×10^6 per well). Then 24 h after seeding, medium was changed to MEM supplemented with 1% charcoal stripped FCS, penicillin (100 U/mL), streptomycin (100 μg/mL), and 2 mM L-glutamate. After an additional 24 h, medium was again changed to MEM now additionally containing the test compounds in DMSO or DMSO alone (final concentration 0.1% DMSO). Cells were incubated with the test compounds for 24 h, harvested, washed with cold PBS, and then directly used for RNA extraction or stored at −80 °C.

RNA Extraction and cDNA Synthesis. Two micrograms of total RNA were extracted from HepG2 or HT-29 cells by the Total RNA Mini Kit from Omega (R6834-02). RNA was reverse transcribed into cDNA using the High-Capacity cDNA Reverse Transcription Kit (Life Technologies: 4368814) according to the manufacturer's protocol.

q-RT PCR. FXR target gene expression was evaluated by quantitative PCR analysis with a StepOnePlus System (Life Technologies) using PowerSYBRGreen (Life Technologies; 12.5 μL per well) and the following primers (300 nM each): SHP, 5′-GCTGTCTGGAGTCCTTCTGG (forward) and 5′-CCAATGATAGGGCGAAAGAAGAG (reverse); CYP7A1, 5′-CACCTTGAGGACGGTTCCTA (forward) and 5′-CGATCCAAAGGGCATGTAGT (reverse); BSEP, 5′-CATGGTGCAAGAAGTGCTGAGT (forward) and 5′-AAGCGATGAGCAACTGAAATGAT (reverse); OSTα, 5′-TGCTGCTCACCAGGAAGAAG (forward) and 5′-ATAGAGCTGTGCTCCCCTCA (reverse); IBABP, 5′-TCAAGGCCACTGTGCAGATG (forward) and 5′-CAGCTTGTCACCCACGATCTC (reverse). Results were normalized to GAPDH *Ct* values. Sequences of the GAPDH primers were as follows: 5′-ATATGATTCCACCCATGGCA (forward) and 5′-GATGATGACCCTTTTGGCTC (reverse). Each sample was set up in duplicate and repeated in at least four independent experiments. The expression was quantified by comparative ΔΔ*Ct* method.

PPAR Transactivation Assay. *Cell Culture.* COS-7 cells were grown in DMEM high glucose, supplemented with 10% FCS, 1 mM sodium pyruvate (SP), penicillin (100 U/mL), and streptomycin (100 μg/mL) at 37 °C and 5% CO_2.

Plasmids for PPAR Transactivation Assay. The Gal4-fusion receptor plasmids pFA-CMV-PPARα-LBD, pFA-CMV-PPARδ-LBD, and pFA-CMV-PPARγ-LBD containing the hinge region and ligand binding domain (LBD) for each of the PPAR subtypes, respectively, were constructed by integrating cDNA fragments obtained from PCR amplification of human monocytes into the *Sma*I/*Xba*I cleavage site of the pFA-CMV vector (Stratagene, La Jolla, CA, USA) and have already been published.[46] The cDNA fragments consist of bps 499−1407 (NM_005 036), bps 412−1323 (NM_006 238) and bps 610−1518 (NM_015 869) for PPARα, PPARδ, and PPARγ, respectively. Frame and sequence of the fusion receptors were verified by sequencing. pFR-Luc (Stratagene) was used as reporter plasmid and pRL-SV40 (Promega) for normalization of transfection efficiency and cell growth.

PPAR Transactivation Assay. The day before transfection, COS-7 cells were seeded in 96-well plates with a density of 30000 cells per well. Transient transfection was carried out using Lipofectamine LTX reagent (Invitrogen, Carlsbad, CA, USA) according to the manufacturer's protocol with pFR-Luc (Stratagene), pRL-SV40 (Promega), and the Gal4-fusion receptor plasmids (pFA-CMV-hPPAR-LBD) of the respective PPAR subtype. Then 5 h after transfection, medium was changed to DMEM without phenol red and 10% FCS, supplemented with 1 mM SP, penicillin (100 U/mL), streptomycin (100 μg/mL), and 2 mM L-glutamate, now additionally containing 0.1% DMSO and the respective test compound or 0.1% DMSO alone as untreated control. Each concentration was tested in triplicate wells, and each experiment was repeated independently at least three times. Following overnight incubation with the test compounds, cells were assayed for luciferase activity using Dual-GloTM luciferase assay system (Promega) according to the manufacturer's protocol. Luminescence was measured with an Infinite M200 luminometer (Tecan Deutschland GmbH). Normalization of transfection efficacy and cell growth was done by division of firefly luciferase data by renilla luciferase data, resulting in relative light units (RLU). Fold activation was obtained by dividing the mean RLU of a test compound at a respective concentration by the mean RLU of untreated control. Relative activation was obtained by dividing the fold activation of a test compound at a respective concentration by the fold activation of PPARα full agonist GW 7647 at 1 μM, PPARδ full agonist L165,041 at 1 μM, or PPARγ full agonist pioglitazone at 1 μM, respectively. EC_{50} and standard error of the mean values were calculated with the mean relative activation values of at least three independent experiments by SigmaPlot 10.0 (Systat Software GmbH) using a four-parameter logistic regression.

TGR5 Assay. The activity of **51** on TGR5 was evaluated by measuring the level of cAMP using a HTR-FRET assay. In brief, NCI-H716 cells were cultured in DMEM supplemented with 10%FBS,

dx.doi.org/10.1021/jm500937v | J. Med. Chem. XXXX, XXX, XXX−XXX

using 96-well plates coated with Matrigel (BD Biosciences). After 24 h, cells were stimulated with increasing concentrations of test compound **51** for 60 min at 37 °C in OptiMEM with 1 mM IBMX (Sigma). The level of intracellular cAMP was assessed using the Lance kit (PerkinElmer) according to the manufacturer's protocol.

Cytotoxicity Assays. *WST-1.* The WST-1 assay from Roche was performed according to manufacturer's protocol. In brief, HepG2 cells were seeded in DMEM supplemented with 1 mM SP, penicillin (100 U/mL), streptomycin (100 μg/mL), and 10% FCS in 96-well plates (3×10^4 cells/well). After 24 h, medium was changed to DMEM supplemented with penicillin (100 U/mL), streptomycin (100 μg/mL), and 1% FCS, and cells were incubated with compound **51** (final concentrations 1, 10, 30, and 100 μM), Revlotron (100 μM) as positive control, and Zileuton (100 μM) and DMEM/1% DMSO as negative controls. After 48 h, WST reagent (Roche) was added to each well according to manufacturer's instructions. After 45 min incubation, absorption (450 nm/reference: 620 nm) was determined with a TEACAN Infinite M200 luminometer. Each experiment was repeated three times in triplicates. Results (expressed as mean ± SEM; $n = 4$; untreated = 100%) **51**: 1 μM, 94 ± 2%; 10 μM, 76 ± 1%; 30 μM, 40 ± 1%; 100 μM, 0%.

LDH. LDH assay (Roche) was performed according to manufacturer's instructions. In brief, HepG2 cells were seeded in DMEM supplemented with 1 mM SP, penicillin (100 U/mL), streptomycin (100 μg/mL), and 10% FCS in 96-well plates (3×10^4 cells/well). After 24 h, medium was changed to DMEM supplemented with penicillin (100 U/mL), streptomycin (100 μg/mL), and 1% FCS, and cells were incubated with the respective compounds for 48 h. As positive control, TRITON X-100 (2%) was added 2 h before measurement. After incubation, supernatant of each well was transferred into a fresh plate and LDH substrate/reagent was added. After 20 min incubation, absorption at measurement (490 nM) and reference (690 nM) wavelength was determined with a TECAN infinite 200. All experiments were performed in triplicates and at least in three independent repeats. Results (expressed as mean ± SEM; $n = 4$; untreated = 0%, Triton X-100 (2%) = 100%) **51**: 1 μM, 0 ± 7%; 10 μM, 0 ± 7%; 30 μM, 63 ± 5%; 100 μM, 91 ± 6%.

Metabolism Assay. The solubilized test compounds (5 μL, final concentration 10 μM in DMSO) were preincubated at 37 °C in 432 μL of phosphate buffer (0.1 M, pH 7.4) together with a 50 μL of NADPH regenerating system (30 mM glucose-6-phosphate, 4 U/mL glucose-6-phosphate dehydrogenase, 10 mM NADP, 30 mM $MgCl_2$). After 5 min, the reaction was started by the addition of 13 μL of microsome mix from the liver of Sprague–Dawley rats (Invitrogen, Darmstadt, Germany; 20 mg protein/mL in 0.1 M phosphate buffer) in a shaking water bath at 37 °C. The reaction was stopped by addition of 250 μL of of ice-cold methanol at 0, 15, 30, and 60 min. The samples were diluted with 250 μL of DMSO and centrifuged at 10000*g* for 5 min at 4 °C. The supernatants were analyzed, and test compounds were quantified by HPLC: mobile phase, MeOH 83%/H_2O 17%/formic acid 0.1%; flow-rate, 1 mL/min; stationary phase, MultoHigh Phenyl phase, 5 μm, 250 × 4 precolumn, phenyl, 5 μm, 20 × 4; detection wavelength, 330 and 254 nm; injection volume, 50 μL. Control samples were performed to check the stability of the compounds in the reaction mixture: first control was without NADPH, which is needed for the enzymatic activity of the microsomes, second control was with inactivated microsomes (incubated for 20 min at 90 °C), third control was without test compounds (to determine the baseline). The amounts of the test compounds were quantified by an external calibration curve, where data are expressed as means ± SEM of single determinations obtained in three independent experiments. The metabolism experiments showed the following curves (expressed as mean ± SEM; $n = 4$) **51**: 0 min, 93.5 ± 2.4%; 15 min, 86.0 ± 1.8%; 30 min, 84.3 ± 1.4%; 60 min, 80.2 ± 0.2%.

■ ASSOCIATED CONTENT

Ⓢ Supporting Information

Preparation and analytical data of intermediate compounds. This material is available free of charge via the Internet at http://pubs.acs.org.

■ AUTHOR INFORMATION

Corresponding Author

*Phone: +49-69-798-29328. Fax: +49-69-798-29332. E-mail: merk@pharmchem.uni-frankfurt.de .

Notes

The authors declare no competing financial interest.

■ ACKNOWLEDGMENTS

We thank Prof. Dr. R. Pellicciari and Dr. D. Passeri for the generous in vitro characterization of compound **51** on TGR5. K.A. gratefully acknowledges financial support from Else Kröner-Fresenius-Stiftung (Dr. Hans Kröner-Graduiertenkolleg) and from CEF.

■ REFERENCES

(1) Fiorucci, S.; Mencarelli, A.; Distrutti, E.; Palladino, G.; Cipriani, S. Targeting farnesoid-X-receptor: from medicinal chemistry to disease treatment. *Curr. Med. Chem.* **2010**, *2*, 139–159.

(2) Fiorucci, S.; Mencarelli, A.; Distrutti, E.; Zampella, A. Farnesoid X receptor: from medicinal chemistry to clinical applications. *Future Med. Chem.* **2012**, *7*, 877–891.

(3) Düfer, M.; Horth, K.; Wagner, R.; Schittenhelm, B.; Prowald, S.; Wagner, T.; Oberwinkler, J.; Lukowski, R.; Gonzalez, F.; Krippeit-Drews, P.; Drews, G. Bile Acids Acutely Stimulate Insulin Secretion of Mouse-Cells via Farnesoid X Receptor Activation and KATP Channel Inhibition. *Diabetes* **2012**, *6*, 1479–1489.

(4) Düfer, M.; Hörth, K.; Krippeit-Drews, P.; Drews, G. The significance of the nuclear farnesoid X receptor (FXR) in β cell function. *Islets* **2012**, *5*, 333–338.

(5) Li, Y.; Jadhav, K.; Zhang, Y. Bile acid receptors in non-alcoholic fatty liver disease. *Biochem. Pharmacol.* **2013**, *11*, 1517–1524.

(6) Adorini, L.; Pruzanski, M.; Shapiro, D. Farnesoid X receptor targeting to treat nonalcoholic steatohepatitis. *Drug Discovery Today* **2012**, *17–18*, 988–997.

(7) Musso, G.; Gambino, R.; Cassader, M. Cholesterol metabolism and the pathogenesis of non-alcoholic steatohepatitis. *Prog. Lipid Res.* **2013**, *1*, 175–191.

(8) Renga, B.; Mencarelli, A.; Vavassori, P.; Brancaleone, V.; Fiorucci, S. The bile acid sensor FXR regulates insulin transcription and secretion. *Biochim. Biophys. Acta* **2010**, *3*, 363–372.

(9) Wang, X.; Fu, X.; van Ness, C.; Meng, Z.; Ma, X.; Huang, W. Bile Acid Receptors and Liver Cancer. *Curr. Pathobiol. Rep.* **2013**, *1*, 29–35.

(10) Nijmeijer, R. M.; Gadaleta, R. M.; van Mil, S. W. C.; van Bodegraven, A. A.; Crusius, J. B.; Dijkstra, G.; Hommes, D. W.; de Jong, D. J.; Stokkers, P. C.; Verspaget, H. W.; Weersma, R. K.; van der Woude, C. J.; Stapelbroek, J. M.; Schipper, M. E.; Wijmenga, C.; van Erpecum, K. J.; Oldenburg, B. Farnesoid X receptor (FXR) activation and FXR genetic variation in inflammatory bowel disease. *PLoS One* **2011**, *8*, e23745.

(11) Hollman, D. A. A.; Milona, A.; van Erpecum, K. J.; van Mil, S. W. C. Anti-inflammatory and metabolic actions of FXR: insights into molecular mechanisms. *Biochim. Biophys. Acta* **2012**, *11*, 1443–1452.

(12) Wildenberg, M. E.; van den Brink, G. R. FXR activation inhibits inflammation and preserves the intestinal barrier in IBD. *Gut* **2011**, *4*, 432–433.

(13) Hageman, J.; Herrema, H.; Groen, A. K.; Kuipers, F. A role of the bile salt receptor FXR in atherosclerosis. *Arterioscler. Thromb. Vasc. Biol.* **2010**, *8*, 1519–1528.

(14) Mencarelli, A.; Fiorucci, S. FXR an emerging therapeutic target for the treatment of atherosclerosis. *J. Cell. Mol. Med.* **2010**, *1*−*2*, 79−92.
(15) Fiorucci, S.; Cipriani, S.; Mencarelli, A.; Renga, B.; Distrutti, E.; Baldelli, F. Counter-regulatory role of bile acid activated receptors in immunity and inflammation. *Curr. Mol. Med.* **2010**, *6*, 579−595.
(16) Silveira, M. G.; Lindor, K. D. Obeticholic acid and budesonide for the treatment of primary biliary cirrhosis. *Expert Opin. Pharmacother.* **2014**, *3*, 365−372.
(17) Mudaliar, S.; Henry, R. R.; Sanyal, A. J.; Morrow, L.; Marschall, H. U.; Kipnes, M.; Adorini, L.; Sciacca, C. I.; Clopton, P.; Castelloe, E.; Dillon, P.; Pruzanski, M.; Shapiro, D. Efficacy and safety of the farnesoid X receptor agonist obeticholic acid in patients with type 2 diabetes and nonalcoholic fatty liver disease. *Gastroenterology* **2013**, *3*, 574−82.e1.
(18) Ryan, K. K.; Tremaroli, V.; Clemmensen, C.; Kovatcheva-Datchary, P.; Myronovych, A.; Karns, R.; Wilson-Pérez, H. E.; Sandoval, D. A.; Kohli, R.; Bäckhed, F.; Seeley, R. J. FXR is a molecular target for the effects of vertical sleeve gastrectomy. *Nature* **2014**, *509*, 183−188.
(19) Merk, D.; Steinhilber, D.; Schubert-Zsilavecz, M. Medicinal chemistry of farnesoid X receptor ligands: from agonists and antagonists to modulators. *Future Med. Chem.* **2012**, *8*, 1015−1036.
(20) Pellicciari, R.; Fiorucci, S.; Camaioni, E.; Clerici, C.; Costantino, G.; Maloney, P. R.; Morelli, A.; Parks, D. J.; Willson, T. M. 6alpha-Ethyl-chenodeoxycholic acid (6-ECDCA), a potent and selective FXR agonist endowed with anticholestatic activity. *J. Med. Chem.* **2002**, *17*, 3569−3572.
(21) Maloney, P. R.; Parks, D. J.; Haffner, C. D.; Fivush, A. M.; Chandra, G.; Plunket, K. D.; Creech, K. L.; Moore, L. B.; Wilson, J. G.; Lewis, M. C.; Jones, S. A.; Willson, T. M. Identification of a Chemical Tool for the Orphan Nuclear Receptor FXR. *J. Med. Chem.* **2000**, *16*, 2971−2974.
(22) Akwabi-Ameyaw, A.; Bass, J. Y.; Caldwell, R. D.; Caravella, J. A.; Chen, L.; Creech, K. L.; Deaton, D. N.; Jones, S. A.; Kaldor, I.; Liu, Y.; Madauss, K. P.; Marr, H. B.; McFadyen, R. B.; Miller, A. B.; Iii, F. N.; Parks, D. J.; Spearing, P. K.; Todd, D.; Williams, S. P.; Wisely, G. B. Conformationally constrained farnesoid X receptor (FXR) agonists: naphthoic acid-based analogs of GW 4064. *Bioorg. Med. Chem. Lett.* **2008**, *15*, 4339−4343.
(23) Chiang, P.; Thompson, D. C.; Ghosh, S.; Heitmeier, M. R. A formulation-enabled preclinical efficacy assessment of a farnesoid X receptor agonist, GW4064, in hamsters and cynomolgus monkeys. *J. Pharm. Sci.* **2011**, *11*, 4722−4733.
(24) Howarth, D. L.; Law, S. H. W.; Law, J. M.; Mondon, J. A.; Kullman, S. W.; Hinton, D. E. Exposure to the synthetic FXR agonist GW4064 causes alterations in gene expression and sublethal hepatotoxicity in eleutheroembryo medaka (*Oryzias latipes*). *Toxicol. Appl. Pharmacol.* **2010**, *1*, 111−121.
(25) Flatt, B.; Martin, R.; Wang, T. L.; Mahaney, P.; Murphy, B.; Gu, X. H.; Foster, P.; Li, J.; Pircher, P.; Petrowski, M.; Schulman, I.; Westin, S.; Wrobel, J.; Yan, G.; Bischoff, E.; Daige, C.; Mohan, R. Discovery of XL335 (WAY-362450), a highly potent, selective, and orally active agonist of the farnesoid X receptor (FXR). *J. Med. Chem.* **2009**, *4*, 904−907.
(26) Singh, N.; Yadav, M.; Singh, A. K.; Kumar, H.; Dwivedi, S. K.; Mishra, J. S.; Gurjar, A.; Manhas, A.; Chandra, S.; Yadav, P. N.; Jagavelu, K.; Siddiqi, M. I.; Trivedi, A. K.; Chattopadhyay, N.; Sanyal, S. Synthetic FXR Agonist GW4064 Is a Modulator of Multiple G Protein-Coupled Receptors. *Mol. Endocrinol.* **2014**, *5*, 659−673.
(27) Merk, D.; Steinhilber, D.; Schubert-Zsilavecz, M. Characterizing ligands for farnesoid X receptor—available in vitro test systems for farnesoid X receptor modulator development. *Expert Opin. Drug Discovery* **2014**, *1*, 27−37.
(28) Merk, D.; Gabler, M.; Gomez, R. C.; Flesch, D.; Hanke, T.; Kaiser, A.; Lamers, C.; Werz, O.; Schneider, G.; Schubert-Zsilavecz, M. Anthranilic acid derivatives as novel ligands for farnesoid X receptor (FXR). *Bioorg. Med. Chem.* **2014**, *8*, 2447−2460.
(29) Achenbach, J.; Gabler, M.; Steri, R.; Schubert-Zsilavecz, M.; Proschak, E. Identification of novel farnesoid X receptor modulators using a combined ligand- and structure-based virtual screening. *Med. Chem. Commun.* **2013**, *6*, 920−924.
(30) Jin, T.; Kitahara, F.; Kamijo, S.; Yamamoto, Y. Copper-catalyzed synthesis of 5-substituted 1*H*-tetrazoles via the [3 + 2] cycloaddition of nitriles and trimethylsilyl azide. *Tetrahedron Lett.* **2008**, *17*, 2824−2827.
(31) Khalafi-Nezhad, A.; Parhami, A.; Soltani Rad, M. N.; Zarea, A. Efficient method for the direct preparation of amides from carboxylic acids using tosyl chloride under solvent-free conditions. *Tetrahedron Lett.* **2005**, *40*, 6879−6882.
(32) Richter, H. G.; Benson, G. M.; Blum, D.; Chaput, E.; Feng, S.; Gardes, C.; Grether, U.; Hartman, P.; Kuhn, B.; Martin, R. E.; Plancher, J. M.; Rudolph, M. G.; Schuler, F.; Taylor, S.; Bleicher, K. H. Discovery of novel and orally active FXR agonists for the potential treatment of dyslipidemia and diabetes. *Bioorg. Med. Chem. Lett.* **2011**, *1*, 191−194.
(33) Akwabi-Ameyaw, A.; Caravella, J. A.; Chen, L.; Creech, K. L.; Deaton, D. N.; Madauss, K. P.; Marr, H. B.; Miller, A. B.; Navas, F., III; Parks, D. J.; Spearing, P. K.; Todd, D.; Williams, S. P.; Wisely, G. B. Conformationally constrained farnesoid X receptor (FXR) agonists: alternative replacements of the stilbene. *Bioorg. Med. Chem. Lett.* **2011**, *20*, 6154−6160.
(34) Di Leva, F. S.; Festa, C.; D'Amore, C.; De Marino, S.; Renga, B.; D'Auria, M. V.; Novellino, E.; Limongelli, V.; Zampella, A.; Fiorucci, S. Binding Mechanism of the Farnesoid X Receptor Marine Antagonist Suvanine Reveals a Strategy To Forestall Drug Modulation on Nuclear Receptors. Design, Synthesis, and Biological Evaluation of Novel Ligands. *J. Med. Chem.* **2013**, *11*, 4701−4717.
(35) De Gottardi, A.; Dumonceau, J. M.; Bruttin, F.; Vonlaufen, A.; Morard, I.; Spahr, L.; Rubbia-Brandt, L.; Frossard, J. L.; Dinjens, W. N.; Rabinovitch, P. S.; Hadengue, A. Expression of the bile acid receptor FXR in Barrett's esophagus and enhancement of apoptosis by guggulsterone in vitro. *Mol. Cancer* **2006**, *5*, 48.
(36) Capello, A.; Moons, L. M.; Van de Winkel, A.; Siersema, P. D.; van Dekken, H.; Kuipers, E. J.; Kusters, J. G. Bile Acid-Stimulated Expression of the Farnesoid X Receptor Enhances the Immune Response in Barrett Esophagus. *Am. J. Gastroenterol.* **2008**, *6*, 1510−1516.
(37) Lee, J. Y.; Lee, K. T.; Lee, J. K.; Lee, K. H.; Jang, K. T.; Heo, J. S.; Choi, S. H.; Kim, Y.; Rhee, J. C. Farnesoid X receptor, overexpressed in pancreatic cancer with lymph node metastasis promotes cell migration and invasion. *Br J. Cancer* **2011**, *6*, 1027−1037.
(38) De Gottardi, A.; Touri, F.; Maurer, C. A.; Perez, A.; Maurhofer, O.; Ventre, G.; Bentzen, C. L.; Niesor, E. J.; Dufour, J. F. The bile acid nuclear receptor FXR and the bile acid binding protein IBABP are differently expressed in colon cancer. *Dig. Dis. Sci.* **2004**, *6*, 982−989.
(39) Journe, F.; Durbecq, V.; Chaboteaux, C.; Rouas, G.; Laurent, G.; Nonclercq, D.; Sotiriou, C.; Body, J. J.; Larsimont, D. Association between farnesoid X receptor expression and cell proliferation in estrogen receptor-positive luminal-like breast cancer from postmenopausal patients. *Breast Cancer Res. Treat.* **2009**, *3*, 523−535.
(40) Silva, J.; Dasgupta, S.; Wang, G.; Krishnamurthy, K.; Ritter, E.; Bieberich, E. Lipids isolated from bone induce the migration of human breast cancer cells. *J. Lipid Res.* **2006**, *4*, 724−733.
(41) Qi, Y.; Jiang, C.; Cheng, J.; Krausz, K. W.; Li, T.; Ferrell, J. M.; Gonzalez, F. J.; Chiang, J. Y. Bile acid signaling in lipid metabolism: metabolomic and lipidomic analysis of lipid and bile acid markers linked to anti-obesity and anti-diabetes in mice. *Biochim. Biophys. Acta* **2014**, *14*, 1388−1981.
(42) Fiorucci, S.; Baldelli, F. Farnesoid X receptor agonists in biliary tract disease. *Curr. Opin. Gastroenterol.* **2009**, *3*, 252−259.
(43) Steri, R.; Achenbach, J.; Steinhilber, D.; Schubert-Zsilavecz, M.; Proschak, E. Investigation of imatinib and other approved drugs as starting points for antidiabetic drug discovery with FXR modulating activity. *Biochem. Pharmacol.* **2012**, *12*, 1674−1681.

(44) Ananthanarayanan, M. Human Bile Salt Export Pump Promoter Is Transactivated by the Farnesoid X Receptor/Bile Acid Receptor. *J. Biol. Chem.* **2001**, *31*, 28857−28865.
(45) Seuter, S.; Väisänen, S.; Rådmark, O.; Carlberg, C.; Steinhilber, D. Functional characterization of vitamin D responding regions in the human 5-lipoxygenase gene. *Biochim. Biophys. Acta* **2007**, *7*, 864−872.
(46) Rau, O.; Wurglics, M.; Paulke, A.; Zitzkowski, J.; Meindl, N.; Bock, A.; Dingermann, T.; Abdel-Tawab, M.; Schubert-Zsilavecz, M. Carnosic acid and carnosol, phenolic diterpene compounds of the labiate herbs rosemary and sage, are activators of the human peroxisome proliferator-activated receptor gamma. *Planta Med.* **2006**, *10*, 881−887.

dx.doi.org/10.1021/jm500937v | *J. Med. Chem.* XXXX, XXX, XXX−XXX